

**Metal-Oxide modified TiO₂ nanostructured thin
films for self-cleaning application in
Photovoltaics**



By

Syeda Izzah Batool Rizvi

Reg No. 00000330653

Session 2020-2022

Supervised by

Dr. Nadia Shahzad

US-Pakistan Center for Advanced Studies in Energy (USPCAS-E)

National University of Sciences and Technology (NUST)

H-12, Islamabad 44000, Pakistan

September 2023

**Metal-Oxide modified TiO₂ nanostructured thin
films for self-cleaning application in
Photovoltaics**



By

Syeda Izzah Batool Rizvi

Reg No.

00000330653

Session 2020-2022

Supervised by

Dr. Nadia Shahzad

**A Thesis Submitted to the US-Pakistan Center for Advanced Studies
in Energy in partial fulfillment of the requirements for the degree of**

**MASTER of SCIENCE in
ENERGY SYSTEMS ENGINEERING**

US-Pakistan Center for Advanced Studies in Energy (USPCAS-E)

National University of Sciences and Technology (NUST)

H-12, Islamabad 44000, Pakistan

September 2023

THESIS ACCEPTANCE CERTIFICATE

Certified that final copy of MS thesis written by Ms. Syeda Izzah Batool Rizvi (Registration No. 00000330653), of U.S.-Pakistan Center for Advanced Studies in Energy has been vetted by undersigned, found complete in all respects as per NUST Statues/Regulations, is within the similarity indices limit and is accepted as partial fulfillment for the award of MS degree. It is further certified that necessary amendments as pointed out by GEC members of the scholar have also been incorporated in the said thesis.

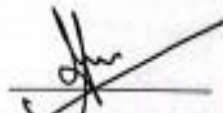
Signature:  _____

Name of Supervisor: Dr. Nadia Shahzad

Date: 13/09/23 _____

Signature (HoD):  _____

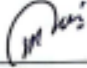

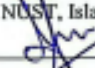


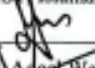
Date: 3/10/23 _____

Signature (Dean/Principal):  _____

Date: 04/10/2023 _____

CERTIFICATE

This is to certify that work in this thesis has been carried out by **Ms. Syeda Izzah Batool Rizvi** and completed under my supervision in Advance Energy and Material Laboratory, US-Pakistan Center for Advanced Studies in Energy (USPCAS-E), National University of Sciences and Technology, H-12, Islamabad, Pakistan.

Supervisor:	 _____ Dr. Nadia Shahzad USPCAS-E NUST, Islamabad
External GEC member 1:	 _____ Dr. M. Imran Shahzad NS & TD (NCP, ISB) NUST, Islamabad
GEC member 2:	 _____ Dr. Ahsan Waqas USPCAS-E NUST, Islamabad
GEC member 3:	 _____ Dr. Rabia Liaquat USPCAS-E NUST, Islamabad
HOD-ESE:	 _____ Dr. Rabia Liaquat USPCAS-E NUST, Islamabad
Dean/Principal:	 _____ Dr. Ahsan Waqas USPCAS-E NUST, Islamabad

Acknowledgement

First and foremost, I would like to express my utmost gratitude to the **Almighty Allah**, The King, and Owner of Dominion and to His **Prophet Muhammad (PBUH)**, who is the city of knowledge, and to **Mola Ali (as)** who is the gate. Without their blessings, this accomplishment would have been unattainable.

I would like to express my heartfelt gratitude to my supervisor **Dr. Nadia Shahzad**, for her invaluable guidance, expertise, and unwavering encouragement. Her mentorship, along with the insightful feedback, and support played a pivotal role in shaping the direction and enhancing the quality of this thesis. I am truly indebted to her for being so understanding, accommodating, and believing in my abilities.

Additionally, I would like to acknowledge my GEC members, for their guidance was of the utmost importance and crucial throughout this research project. I appreciate the assistance from my lab engineers and my lab fellows from Advance Energy and Materials Lab (AEMS) and Solar Energy Research Lab, for always being there to cheer me on even in the most difficult times.

I would like to thank USPCAS-E for providing exceptional lab facilities as the resources and equipment provided played a significant role in the success of this research endeavour. Access to such excellent facilities helped me in gathering the necessary data for the research.

This thesis is the testament of a team effort, and I am grateful that you all supported me along the way.

Izzah Batool

Dedication

To my loving parents, the driving force behind my academic pursuits. I am forever indebted to them for their sacrifices, constant prayers and for being my pillars of strength throughout this journey and my life in general.

To my beloved siblings, for their support and camaraderie that kept me motivated and determined.

To my husband, for his understanding, patience and encouragement that allowed me to focus on my research.

To my friends, for being on my side always.

Abstract

Solar energy is still one of the appealing energy sources despite its variable availability based on the time and location. Keeping surfaces clean and preventing the buildup of dust and other pollutants is crucial for improving the effectiveness of solar energy conversion devices, such as photovoltaic panels. Self-cleaning surfaces have achieved success in the environmental and energy sectors recently. These surfaces are employed, in particular, in the solar energy sector to prevent the buildup of dirt on photovoltaic (PV) modules.

In this study, optically transparent, hydrophilic Silica (SiO₂) modified Titania (TiO₂) nanofibrous thin films have been synthesized on glass substrates via using electrospinning technique for self-cleaning application in a solar cell. The coatings were prepared by varying the TiO₂-SiO₂ ratio as (3:1, 1:1, 1:3). TiO₂-SiO₂ formulated ratio (1:1) outperformed in comparison to other formulations and was found to have a crystalline nature with randomly orientated network of fibers having diameter in the range 88-95nm. FTIR spectroscopy confirms complete evaporation of polyvinylpyrrolidone (PVP) from temperature annealed sample. The electrospun TiO₂-SiO₂ (1:1) nanofibers showed hydrophilic nature with water contact angle (WCA) of 11.3°. The Soiling study was performed under different tilt angles of 0°, 33.4° and 60°. Upon soiling the coating showed >16% enhancement in optical transmittance than the glass substrate. Soiling density decreased up to 38.9%, and to 64.9% in comparison to uncoated substrate that showed 9.08%, and 22.2% and the photovoltaic (PV) efficiency was improved by 0.8% and 1% for tilt angles of 33.4° and 60° respectively.

Keywords: *Solar cells, Self-cleaning coatings, Anti-soiling, Titanium Dioxide, Silicon Dioxide, Electrospinning, Nanofibers, Hydrophilic*

Table of Contents

Abstract	vii
List of Figures	xii
List of Tables	xiv
Publication	xv
List of Abbreviations	xvi
Chapter: 1 Introduction	1
1.1. Sustainable Energy Transition	1
1.1.1 Solar Energy as Solution	1
1.2. Soiling on PV Modules	2
1.3. Factors Effecting Soiling on PV Module	2
1.4. Methodologies to Study Soiling on PV Modules	3
1.4.1. Natural Soiling	3
1.4.2. Artificial Soiling.....	3
1.5. Cleaning Methods for PV Modules.....	3
1.5.1. Mechanical Cleaning.....	4
1.5.2. Electrostatic Cleaning	4
1.5.3. Surface Treatment	4
1.6. Self-Cleaning Mechanism	5
1.6.1. Photo-Induced Hydrophilic/Superhydrophilic Coatings.....	6
1.6.2. Hydrophobic/Superhydrophobic Coatings.....	7
1.7. Self-Cleaning Coatings.....	8
1.8. Problem Statement	8
1.9. Proposal	9
1.10. Scope	9
1.11. Limitation	9
1.12. Objectives.....	9
Summary	9

References	11
Chapter: 2 Literature Review	14
2.1. Self-Cleaning Materials.....	14
2.1.1. TiO ₂	14
2.1.2. SiO ₂	14
2.1.3. ZrO ₂	15
2.1.4. Al ₂ O ₃	15
2.1.5. ZnO.....	15
2.1.6. Polymer Coatings	15
2.2. Performance of Self-Cleaning Materials.....	16
2.2.1. TiO ₂	16
2.2.2. Modified TiO ₂	16
2.2.3. SiO ₂	17
2.2.4. SiO ₂ -TiO ₂	17
2.3. Synthesis and Fabrication of Anti-Soiling Coatings.....	18
2.3.1. Sol-Gel Route.....	18
2.3.1.1. Dip-Coating.....	19
2.3.1.2. Spin Coating.....	20
2.3.1.3. Spray Coating.....	21
2.4. Performance Studies in Outdoor Conditions.....	23
2.5. Performance Studies in Indoor Conditions	24
Summary	25
References	27
Chapter: 3 Introduction to Deposition, Characterization and Anti-Soiling Testing	35
3.1. Deposition	35
3.1.1. Electrospinning.....	35
3.1.2. Plasma Cleaning.....	36

3.2. Characterization	37
3.2.1. X-Ray Diffraction (XRD)	37
3.2.2. UV-VIS-NIR Spectroscopy.....	38
3.2.3. Scanning electron Microscopy (SEM)	40
3.2.4. Fourier Transform Infrared spectroscopy (FTIR)	41
3.2.5. Water Contact Angle (WCA).....	42
3.3. Anti-Soiling Testing.....	43
3.3.1. Indoor Soiling Chamber	43
3.3.2. IV-Curve Measurement using Solar Simulator	44
Summary	45
References	46
Chapter: 4 Experimental Work	47
4.1. Materials.....	47
4.2. Preparation of the precursor solution for Electrospinning	47
4.3. Substrate Preparation.....	48
4.4. Fabrication of TiO ₂ -SiO ₂ Nanofibers	48
4.5. Film Characterizations	49
4.6. Anti-Soiling Testing.....	50
4.6.1. Soiling	50
4.6.2. IV-Curve Measurement.....	50
Flow chart.....	51
Summary	51
Chapter: 5 Results and Discussion	53
5.1. Structural Analysis	53
5.2. Transmittance Results	54
5.3. Chemical Analysis.....	56
5.4. Wettability Study.....	57
5.5. Morphological Analysis	57

5.6. Soiling Study in Indoor Conditions.....	59
5.6.1. Analysis of soiling density under different tilt angles.....	59
5.6.2. Analysis of direct transmittance after soiling.....	60
5.6.3 I-V characteristics and Current Density Analysis.....	61
5.7. Comparison of this study with the reference studies.....	64
Summary	64
References	66
Chapter: 6 Conclusion and Recommendations	69
6.1. Conclusion.....	69
6.2. Recommendations	69
Summary	70
Appendix-A: Journal Article.....	71

List of Figures

Figure 1.1. Factors effecting dust settlement.....	2
Figure 1.2. Key components of PV module	5
Figure 1.3. Self-cleaning performance based on wettability.....	6
Figure 1.4. Photoexcitation of self-cleaning coatings.....	7
Figure 1.5. Rolling and sliding motion of water droplets	8
Figure 2.1. Schematic showing the process of Dip-coating.....	19
Figure 2.2. Graphical Illustration of spin coating	21
Figure 2.3. Schematics of spray coating method	22
Figure 3.1. Schematic diagram of a conventional electrospinning setup.....	36
Figure 3.2. Plasma Cleaning setup.....	37
Figure 3.3. Schematic diagram of X-ray diffraction	38
Figure 3.4. Schematics of UV-VIS-NIR spectroscopy	39
Figure 3.5. Schematic diagram of SEM	41
Figure 3.6. Schematic diagram of FTIR	42
Figure 3.7. Schematic diagram and setup of water contact angle measurement.....	43
Figure 3.8. Setup of Indoor Soiling Chamber.....	44
Figure 3.9. Oriel Sol3A simulator.....	44
Figure 4.1. Electrospinning solution of a) TiO ₂ b) TiO ₂ -SiO ₂ composite.....	48
Figure 4.2. Schematic showing nanofiber fabrication through electrospinning	49
Figure 4.3. Schematic showing the setup of indoor soiling chamber	50
Figure 5.1. XRD plots of the annealed thin films at 500 °C	53
Figure 5.2. Optical transmittance and Tauc plot curves obtained after 3 mins (a, b) and 5 mins (c, d) of electrospinning.....	55
Figure 5.3. FTIR spectra of temperature non-annealed and annealed TiO ₂ -SiO ₂ (1:1) nanofibrous thin film.....	56
Figure 5.4. Water contact angle measurements of TiO ₂ and TiO ₂ -SiO ₂ thin films....	57
Figure 5.5. SEM images of a) TiO ₂ , c) TiO ₂ -SiO ₂ (3:1), e) TiO ₂ -SiO ₂ (1:1), g) TiO ₂ - SiO ₂ (1:3) nanofibrous thin films and their respective close view b, d, f and h) and Elemental mapping results above.....	58
Figure 5.6. Soil deposition density vs Tilt angle.....	59

Figure 5.7. Optical transmittance results of a) TiO ₂ , b) TiO ₂ -SiO ₂ (3:1), c) TiO ₂ -SiO ₂ (1:1) d) TiO ₂ -SiO ₂ (1:3) obtained after soiling under tilt angles of 0°, 33.4° and 60°	61
Figure 5.8. I-V curves for the TiO ₂ -SiO ₂ films under tilt angles of 0°, 33.4° and 60°	62
Figure 5.9. Current density analysis of the developed coatings for all three tilt angles	63

List of Tables

Table 1.1. The summary of the water contact angle and transmittance enhancement of the coatings before and after soiling.	64
--	----

Publication

Izzah Batool; Nadia Shahzad; Roha Shahzad; Aamir Naseem Satti; Rabia Liaquat; Muhammad Imran Shahzad; Adeel Waqas “**Self-Cleaning study of SiO₂ modified TiO₂ nanofibrous thin films via Electrospinning for application in solar cell**”, *Solar Energy* (**Under Review**).

List of Abbreviations

SDGs	Sustainable development goals
PV	Photovoltaics
EVA	Ethylene vinyl acetate
PVB	Polyvinyl butyral
TPO	Thermoplastic polyolefins
TiO ₂	Titanium dioxide
OTS	Octadecyltrichlorosilane
CVD	Chemical vapor deposition
HMDS	Hexamethyldisilazane
AS	Anti-soiling
PM	Particulate matter
AR	Anti-reflective
LED	Light emitting diode
WCA	Water contact angle

Chapter: 1 Introduction

1.1. Sustainable Energy Transition

SDG 7, one of the Sustainable Development Goals established by United Nation's, adopted in 2015, lays a major emphasis on tackling global energy concerns. This objective is made up of three important targets that aim to bring about good change in the energy industry. To begin, it seeks to ensure that all citizens, regardless of geographical location or economic level, have access to inexpensive, dependable, and contemporary energy services. Second, SDG 7 asks for a significant rise in the amount of renewable energy sources in the global energy mix, recognizing their critical role in climate change mitigation and sustainable development. Finally, the target aims to double the pace of increase in global energy efficiency, recognizing the necessity of optimizing energy usage to decrease waste and environmental damage. SDG 7 strives to create a thorough change in the energy sector that is aligned with sustainability and supports a more equitable and greener future by concentrating on these objectives[1].

Due to annual population growth, world energy demand as well as consumption have grown dramatically. Toxic gases emitted by conventional fossil fuels, as well as the fuel's ongoing depletion, have stimulated interest in ecologically benign and renewable energy sources[2]. Sustainable energy transition to renewable sources such as photovoltaics can be the answer to the rising demand for energy while also reducing the impact of produced hazardous emissions and the environmental degradation that comes with it[3].

1.1.1 Solar Energy as Solution

Presently, the almost plentiful and clean source is Solar energy. It is one of the most excellent source because of its accessibility and safety. Solar photovoltaic (PV) technology is widely valued due to its ability to transform solar light into electric energy via photoelectric effects[4]. Solar power generation is becoming more popular across the world, and it is expanding both technologically and financially. As a result, efforts in research and development must continue to keep up with the latest innovations. This enables solar energy to meet the requirements of future generations while also making accepted technology more dependable[2].

1.2. Soiling on PV Modules

With ever-increasing technological innovation to exploit solar energy in the modern day, the sustainability of such energy devices has been a major worry in recent years. Solar panels frequently become filthy because of dust, grime, organic particle matter, and other inorganic pollutant accumulation on their surface over time. This, in turn, significantly affects the efficiency of the solar panels. It has also been shown that in some areas, efficiency loss might be as high as 25%-30% [5]. However, dust collection concerns can reduce the effectiveness of PV panels installed, especially when dust storms are frequent, and water is scarce [6]. Practically, the effectiveness of PV panels in deserts is strongly linked to their anti-soiling properties [7]. Unwanted dust accumulation would shield PV panels from solar light irradiation, resulting in statistically significant power production reductions [8][9]. Evidently, Sharma and Chandel observed a 70% drop in power efficiency when comparing an uncleaned, dust-accumulated PV system to a regularly cleaned PV system [10]. This research revealed the significance of dust reduction in maintaining high photoelectric conversion efficiency of PV panels.

1.3. Factors Effecting Soiling on PV Module

It has been shown that dust buildup is mostly determined by slope, orientation, kind of coating, surface roughness, and so on. The following factors influence dust settlement: as indicated in Figure 1.1.

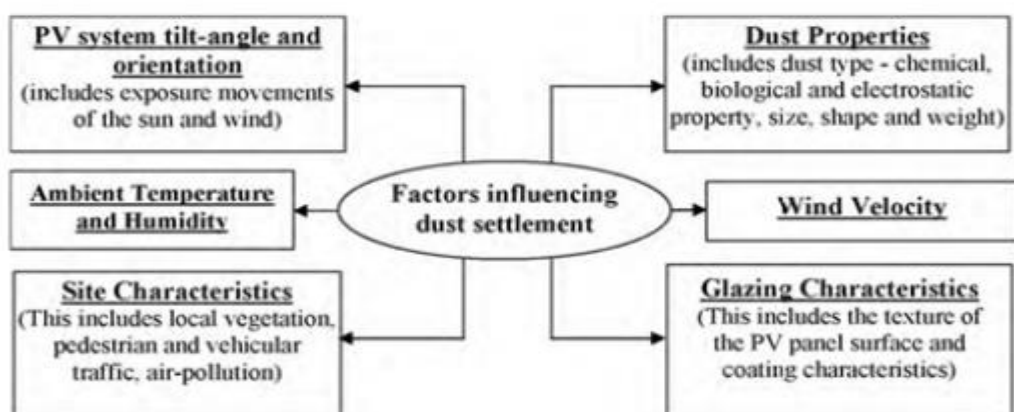


Figure 1.1. Factors effecting dust settlement [11]

It has been found that energy losses in fixed horizontal panels range from 8 to 22% as compared to tilted panels (45°), where losses range from 1-8%[11]. Other external components such as humidity, temperature, wind speed, and geographical features such as traffic, air pollution, and plants all play important roles in dust deposition. Furthermore, the biological, electrostatic, and chemical characteristics of dust, as well as the shape, size, and weight of dust particles, impact dust buildup on panel surfaces[12]. Several investigations have been undertaken on the process of dust deposition on PV modules. The dust buildup density is found to be mostly dependent on the angle at which the PV module is mounted[11]. The dust buildup blocked sunlight penetration through the photovoltaic module glass cover, reducing sunlight reaching the solar cell significantly. Power loss due to soiling would vary depending on the physical and chemical characteristics of dust particles, as well as geographical location[13].

1.4. Methodologies to Study Soiling on PV Modules

The methods to study soiling consists of natural and artificial soiling. The effect in both cases can be studied either by analyzing the optical properties or through the measurement of short circuit current and open circuit voltage i.e., the electrical properties.

1.4.1. Natural Soiling

The natural soiling of PV panels happens when the panels are located near regions where there are trees also in desert areas. The dust particles on solar panels are collected when they are exposed to air pollution, agriculture construction areas, bird droppings and due to vehicular movement[14].

1.4.2. Artificial Soiling

Artificial soiling of PV panels is performed to investigate the influence of soiling on the electrical and optical properties of PV panels. In the laboratory, dust samples will be manufactured, or dust collected from outside can be put on PV panels in homemade soiling stations within controlled environmental conditions. When compared to natural soiling, artificial soiling study is a quick process[14].

1.5. Cleaning Methods for PV Modules

Various cleaning techniques have been employed including mechanical, automated, and self-cleaning coatings. The methods are discussed below.

1.5.1. Mechanical Cleaning

The mechanical approach includes the method of brushing, blowing and ultrasonic vibrations. Brushing cleans the solar panel using a broom or brush powered by human or machine energy. In comparison to human energy, machines can clean up solar panels quickly and efficiently. Aside from brushing, the blowing method uses air-blowing and water-spraying to clean the solar panel. Air-blowing blasts dust and contaminants away from the solar panel at a certain air velocity, removing the hot thermal air on the solar surface. The water-spraying approach works in the same way as the air-blowing method. Because of their capacity to cool the solar surface and manage the cracking effect, both procedures may be employed in high humidity and high temperature environments. Wiper provides an effective option for removing impurities from the surface of a solar panel, with the wiper being operated by a linear piezoelectric actuator via vibration. To move the wiper back and forth across the solar panel, the resonance frequency and amplitude voltage must be adjusted. To create the mechanical movement of cleaning wipers, spray nozzles, power is employed on PV panels for the mechanical approach[13].

1.5.2. Electrostatic Cleaning

Electrostatic dust removal is one example of an electric approach. Gaofa et al. [1] proposed two ways for charging particles on the moon. 1) Electrons released from the surface of particles because of photoemissions caused by UV radiation 2) Charging via triboelectric means. Electrostatic forces draw both charged and uncharged dust to solar panels with high potential surfaces. The solar panel will charge the dust particles. Due to electrostatic forces, they will repel one another because they have the same electric charge. Finally, solar panels discharge dust particles. The PV system is constrained by this method because of the impact of rain. The electric curtain method is another well-known electro dust reduction technology. To reject lunar and Mars dust at low pressure, the electrostatic approach requires electricity to generate triboelectric charging and dielectric forces on parallel electrodes, commonly wire and copper electrodes. However, this electrostatic barrier is ineffectual for earth climate change, particularly on wet days, and cannot be used on a wide scale with PV panels[11].

1.5.3. Surface Treatment

The surface treatment of PV module glass cover with thin coating layer(s) can protect absorbents and reflectors from corrosion, dust, and optical losses. Self-cleaning

coatings make it easier to remove dust from PV module, increasing their output power. Solar panel coatings that improve self-cleaning include two types of films: superhydrophilic and superhydrophobic films. Self-cleaning nano-films are being studied as suitable coatings for enhancing PV module output power[15]. They can be differentiated based on their wettability: superhydrophobicity in the Lotus effect and photocatalytic hydrophilicity, both of which are mainly dependent on TiO_2 . Indeed, both surface characteristics aid in the self-cleaning properties of the underlying substrates. Superhydrophobic surfaces have a WCA of more than or equal to 150° , allowing spherical water droplets to be readily rolled onto the surface, carrying away dust and dirt, whereas superhydrophilic surfaces have a lower $\text{WCA} < (5^\circ)$, allowing complete spreading of water onto them, easily carrying dust particles as it flows[16] .

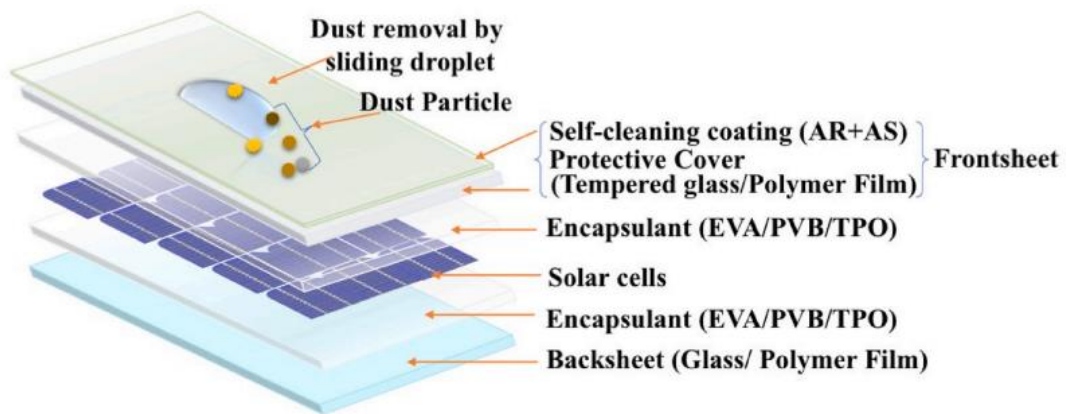


Figure 1.2. Key components of PV module [17]

1.6. Self-Cleaning Mechanism

The lotus flower (*Nelumbo*) leaf is where the self-cleaning mechanism was first discovered. It was discovered that dirt particles were removed from the surface by the water droplets because the surface of such leaves contains a nanostructure that restricts the water droplet's attachment to it. Later, the precise process was discovered in the wings of various insects and other plants, including cane, nasturtium, and prickly pear. The name "lotus effect" was first used by Barthlott and Ehler to characterize these self-cleaning properties when they did the early research on the self-cleaning of surfaces. Self-cleaning coatings mainly produce water droplets in the form of balls that can remove dust from their surface either through hydrophilic or hydrophobic action. These layers allow for a variety of water contact angles, which helps the molecules

spread across the surface or glide and roll. Many surfaces are now being given stronger self-cleaning abilities by carefully studying the characteristics of the materials and the circumstances in which they work best[18].

As stated earlier, two different types of self-cleaning methods are available:

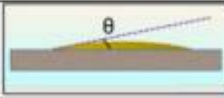


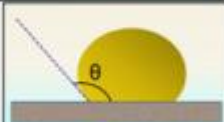

Wettability	Contact angle	Droplet schematic	Hydrophobicity
Super hydro-phallic	$\theta < 10^\circ$		
Hydrophilic	$10^\circ < \theta < 90^\circ$		
Hydrophobic	$90^\circ > \theta > 150^\circ$		
Super hydro-phobic	$150^\circ > \theta > 180^\circ$		

Figure 1.3. Self-cleaning performance based on wettability[19]

1.6.1. Photo-Induced Hydrophilic/Superhydrophilic Coatings

When using a superhydrophilic coating, water is forced to spread over the surfaces (water sheeting), which removes dirt and other impurities. In contrast, when using a superhydrophobic coating, water droplets roll and glide over the surfaces, cleaning them. Using the right metal oxides, superhydrophilic coatings have the extra ability to chemically degrade the intricate dirt buildups through sunlight-assisted cleaning processes (photocatalysis).

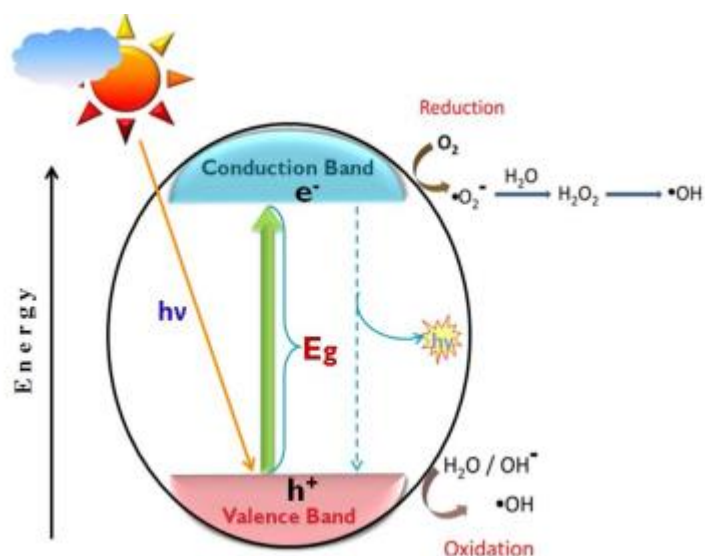


Figure 1.4. Photoexcitation of self-cleaning coatings[20]

Numerous research teams have been studying photocatalysis extensively for many years, and the process is quite well understood. Electron-hole pairs can be excited by UV light since TiO_2 is a semiconductor. The photogenerated holes then combine with water to make hydroxyl ($-\text{OH}$) radicals, while the photogenerated electrons react with molecular oxygen (O_2) to produce superoxide radical anions ($\cdot\text{O}_2^-$). Together, these two reactive radicals break down organic substances. The separation of electrons and holes is improved by the $-\text{OH}$ groups, which can trap more photogenerated holes and increase photocatalysis[21].

1.6.2. Hydrophobic/Superhydrophobic Coatings

The water contact angle (WCA) of the hydrophobic coated surface is 90° , and it has a low surface energy. Superhydrophobic characteristics are indicated by a water contact angle (WCA) higher than 150° . Because of the nonequilibrium thermodynamic condition of a superhydrophobic surface, suspended water, dirt, or any pollutant rolls down spontaneously. They can also help to reduce corrosion and ice formation, as well as drag[22][23]. Fig 1.2. describes the motion of the water droplet for both hydrophobic and superhydrophobic coatings.

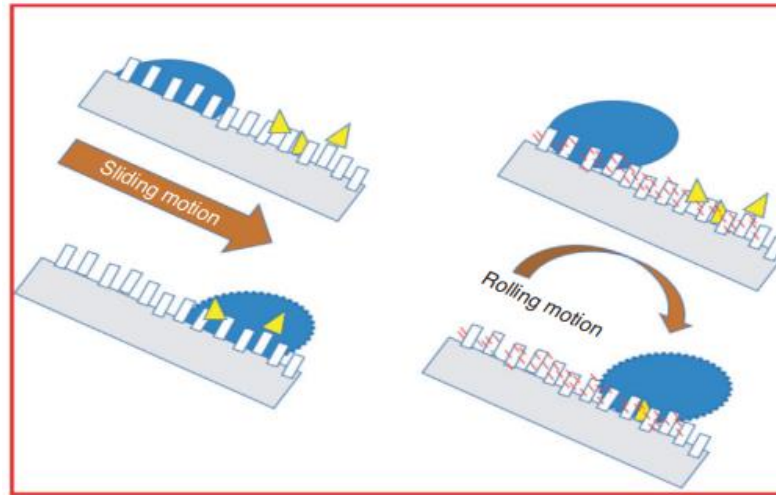


Figure 1.5. Rolling and sliding motion of water droplets [24]

Hydrophobic coatings remove dust by a sliding motion of a half- spherical droplet while superhydrophobic coating removes dust via a rolling down motion of a spherical droplet[24].

The wetting behavior of hydrophobic and hydrophilic coatings is the result of a combination of surface morphology, surface free energy, and chemical composition. Semiconductive metal oxide can be utilized as a self-cleaning coating[22].

1.7. Self-Cleaning Coatings

Self-cleaning coatings are frequently applied to solar cells, outside building windows, glasses, automotive windows, textiles, and clothing. TiO_2 , SiO_2 , ZrO_2 , Al_2O_3 , ZnO , and polymer coatings are among the self-cleaning materials that have been mostly explored. Due to its capacity to clean surfaces through two unique properties— photocatalysis and superhydrophilicity— TiO_2 has been the major subject of research in self-cleaning applications. However, other materials could not surpass the properties of TiO_2 [21].

1.8. Problem Statement

Self-cleaning coatings are critical for reducing dust adherence on solar cover glass and, as a result, increasing the power efficiency of solar modules. As a self-cleaning coating, titanium dioxide is often utilized. However, TiO_2 's transparency is hampered by its comparatively low band gap of 3.2 eV (anatase phase). For solar cover glass applications, this transparency is critical. TiO_2 also loses its photo-induced hydrophilicity, which is responsible for its self-cleaning feature, when exposed to

darkness. Furthermore, evaluating the effectiveness of coatings outside for self-cleaning is difficult since conditions are unpredictable.

1.9. Proposal

By combining TiO_2 with metal oxides with a large band gap, such as silica, the transparency of TiO_2 can be increased. Furthermore, the addition of SiO_2 results in the formation of hydroxyl groups on the glass surface, resulting in a very hydrophilic surface. This hydrophilicity helps to increase the self-cleaning characteristic. Furthermore, the composite coatings' self-cleaning ability can be analyzed by testing them in a controlled indoor soiling chamber where the conditions can be properly maintained and monitored.

1.10. Scope

Improve the self-cleaning capability of TiO_2 - SiO_2 nanofibrous coatings on a prototype small-scale PV module.

1.11. Limitation

Due to instrumental limitation, not tested for large area substrate.

1.12. Objectives

- Synthesis of metal-oxide modified TiO_2 nanostructured composite coatings by electrospinning.
- Characterization of the developed coatings to study their optical, structural, and morphological properties.
- Reliability testing of developed optimized coatings for their self-cleaning property in a homemade soiling chamber.

Summary

The introduction emphasizes the significance of a sustainable energy transition, as well as the role of solar energy as a solution. It emphasizes the issue of soiling on PV modules, which can have a substantial impact on their efficiency. The elements that influence soiling are explored, including slope, orientation, coating, and dust characteristics. The approaches for studying soiling, both natural and artificial, are discussed. Mechanical cleaning, electrostatic cleaning, and surface treatment are all stated as cleaning procedures for PV modules. Self-cleaning coatings are introduced,

with a focus on hydrophilic/superhydrophilic and hydrophobic/superhydrophobic coatings. TiO_2 , SiO_2 , ZrO_2 , Al_2O_3 , ZnO , and polymer coatings are among the self-cleaning materials explored. In the end, the issues with TiO_2 coatings are highlighted and proposed solutions to overcome them are discussed with research objectives. Overall, the introduction gives a thorough review of the significance of renewable energy, the issues of soiling on PV modules, and the possible solutions presented by self-cleaning coatings and materials.

References

- [1] E. Fares, M. Buffiere, B. Figgis, Y. Haik, and R. J. Isaifan, “Soiling of photovoltaic panels in the Gulf Cooperation Council countries and mitigation strategies,” *Solar Energy Materials and Solar Cells*, vol. 231. Elsevier B.V., Oct. 01, 2021. doi: 10.1016/j.solmat.2021.111303.
- [2] T. Salamah *et al.*, “Effect of dust and methods of cleaning on the performance of solar PV module for different climate regions: Comprehensive review,” *Science of the Total Environment*, vol. 827. Elsevier B.V., Jun. 25, 2022. doi: 10.1016/j.scitotenv.2022.154050.
- [3] C. Ghenai, T. Salameh, and A. Merabet, “Technico-economic analysis of off grid solar PV/Fuel cell energy system for residential community in desert region,” *Int J Hydrogen Energy*, vol. 45, no. 20, pp. 11460–11470, Apr. 2020, doi: 10.1016/j.ijhydene.2018.05.110.
- [4] Z. S. Huang *et al.*, “Experimental investigation of the anti-soiling performances of different wettability of transparent coatings: Superhydrophilic, hydrophilic, hydrophobic and superhydrophobic coatings,” *Solar Energy Materials and Solar Cells*, vol. 225, Jun. 2021, doi: 10.1016/j.solmat.2021.111053.
- [5] D. Adak *et al.*, “Self-cleaning V-TiO₂:SiO₂ thin-film coatings with enhanced transmission for solar glass cover and related applications,” *Solar Energy*, vol. 155, pp. 410–418, 2017, doi: 10.1016/j.solener.2017.06.014.
- [6] L. zhi Zhang, A. jian Pan, R. rong Cai, and H. Lu, “Indoor experiments of dust deposition reduction on solar cell covering glass by transparent super-hydrophobic coating with different tilt angles,” *Solar Energy*, vol. 188, pp. 1146–1155, Aug. 2019, doi: 10.1016/j.solener.2019.07.026.
- [7] B. Hammad, M. Al-Abed, A. Al-Ghandoor, A. Al-Sardeah, and A. Al-Bashir, “Modeling and analysis of dust and temperature effects on photovoltaic systems’ performance and optimal cleaning frequency: Jordan case study,” *Renewable and Sustainable Energy Reviews*, vol. 82. Elsevier Ltd, pp. 2218–2234, Feb. 01, 2018. doi: 10.1016/j.rser.2017.08.070.

- [8] K. K. Ilse, B. W. Figgis, V. Naumann, C. Hagendorf, and J. Bagdahn, “Fundamentals of soiling processes on photovoltaic modules,” *Renewable and Sustainable Energy Reviews*, vol. 98, pp. 239–254, Dec. 2018, doi: 10.1016/j.rser.2018.09.015.
- [9] M. S. Mozumder, A. H. I. Mourad, H. Pervez, and R. Surkatti, “Recent developments in multifunctional coatings for solar panel applications: A review,” *Solar Energy Materials and Solar Cells*, vol. 189, pp. 75–102, Jan. 2019, doi: 10.1016/j.solmat.2018.09.015.
- [10] V. Sharma and S. S. Chandel, “Performance and degradation analysis for long term reliability of solar photovoltaic systems: A review,” *Renewable and Sustainable Energy Reviews*, vol. 27, pp. 753–767, 2013. doi: 10.1016/j.rser.2013.07.046.
- [11] S. V S and D. S. K, “Solar Photovoltaic Panels Cleaning Methods A Review,” 2018. [Online]. Available: <http://www.acadpubl.eu/hub/>
- [12] I. Arabatzis *et al.*, “Photocatalytic, self-cleaning, antireflective coating for photovoltaic panels: Characterization and monitoring in real conditions,” *Solar Energy*, vol. 159, pp. 251–259, Jan. 2018, doi: 10.1016/j.solener.2017.10.088.
- [13] A. Syafiq, A. K. Pandey, N. N. Adzman, and N. A. Rahim, “Advances in approaches and methods for self-cleaning of solar photovoltaic panels,” *Solar Energy*, vol. 162. Elsevier Ltd, pp. 597–619, Mar. 01, 2018. doi: 10.1016/j.solener.2017.12.023.
- [14] A. Shaju and R. Chacko, “Soiling of photovoltaic modules- Review,” in *IOP Conference Series: Materials Science and Engineering*, Institute of Physics Publishing, Aug. 2018. doi: 10.1088/1757-899X/396/1/012050.
- [15] C. Atkinson, C. L. Sansom, H. J. Almond, and C. P. Shaw, “Coatings for concentrating solar systems - A review,” *Renewable and Sustainable Energy Reviews*, vol. 45. Elsevier Ltd, pp. 113–122, 2015. doi: 10.1016/j.rser.2015.01.015.
- [16] M. S. Mozumder, A. H. I. Mourad, H. Pervez, and R. Surkatti, “Recent developments in multifunctional coatings for solar panel applications: A review,” *Solar Energy Materials and Solar Cells*, vol. 189, pp. 75–102, Jan. 2019, doi: 10.1016/j.solmat.2018.09.015.
- [17] D. Adak, R. Bhattacharyya, and H. C. Barshilia, “A state-of-the-art review on the multifunctional self-cleaning nanostructured coatings for PV panels, CSP mirrors and

related solar devices,” *Renewable and Sustainable Energy Reviews*, vol. 159. Elsevier Ltd, May 01, 2022. doi: 10.1016/j.rser.2022.112145.

- [18] V. T. Lukong, K. Ukoba, and T. C. Jen, “Review of self-cleaning TiO₂ thin films deposited with spin coating,” *International Journal of Advanced Manufacturing Technology*, vol. 122, no. 9–10. Springer Science and Business Media Deutschland GmbH, pp. 3525–3546, Oct. 01, 2022. doi: 10.1007/s00170-022-10043-3.
- [19] T. Salamah *et al.*, “Effect of dust and methods of cleaning on the performance of solar PV module for different climate regions: Comprehensive review,” *Science of the Total Environment*, vol. 827. Elsevier B.V., Jun. 25, 2022. doi: 10.1016/j.scitotenv.2022.154050.
- [20] N. T. Padmanabhan and H. John, “Titanium dioxide based self-cleaning smart surfaces: A short review,” *Journal of Environmental Chemical Engineering*, vol. 8, no. 5. Elsevier Ltd, Oct. 01, 2020. doi: 10.1016/j.jece.2020.104211.
- [21] V. A. Ganesh, A. S. Nair, H. K. Raut, T. M. Walsh, and S. Ramakrishna, “Photocatalytic superhydrophilic TiO₂ coating on glass by electrospinning,” *RSC Adv*, vol. 2, no. 5, pp. 2067–2072, Mar. 2012, doi: 10.1039/c2ra00921h.
- [22] S. Nundy, A. Ghosh, and T. K. Mallick, “Hydrophilic and Superhydrophilic Self-Cleaning Coatings by Morphologically Varying ZnO Microstructures for Photovoltaic and Glazing Applications,” *ACS Omega*, vol. 5, no. 2, pp. 1033–1039, Jan. 2020, doi: 10.1021/acsomega.9b02758.
- [23] G. G. Jang, D. B. Smith, G. Polizos, L. Collins, J. K. Keum, and D. F. Lee, “Transparent superhydrophilic and superhydrophobic nanoparticle textured coatings: Comparative study of anti-soiling performance,” *Nanoscale Adv*, vol. 1, no. 3, pp. 1249–1260, 2019, doi: 10.1039/c8na00349a.
- [24] A. Syafiq *et al.*, “Application of transparent self-cleaning coating for photovoltaic panel: a review,” *Current Opinion in Chemical Engineering*, vol. 36. Elsevier Ltd, Jun. 01, 2022. doi: 10.1016/j.coche.2022.100801.

Chapter: 2 Literature Review

2.1. Self-Cleaning Materials

Material such as semiconductor metal-oxides are widely employed as self-cleaning coatings on PV cover glass because of their various advantages including wide bands, photocatalytic efficiency, environmental friendliness etc. Some of them are discussed below.

2.1.1. TiO₂

Titanium dioxide has three distinct crystal structures: anatase, rutile, and brookite. When compared to rutile or brookite, anatase is a structure with strong photocatalytic characteristics. When synthesizing TiO₂, it is critical to pay close attention to factors such as crystal structure, shape, and phase stability[1]. TiO₂ provides both photocatalysis, which is responsible for breakdown of organic pollutants, and photo-induced superhydrophilicity, which facilitates the washing of organic pollutants off the surface by rain[2]. Titania, in addition to its hydrophilic qualities and strong photo reactivity, has long-term stability, superior mechanical and chemical properties, high heat resistance, and low toxicity and costs[3].

2.1.2. SiO₂

Silicon dioxide can exhibit photocatalytic properties when exposed to ultraviolet (UV) light. This means that when sunlight or UV radiation hits the SiO₂-coated surface, it can initiate a chemical reaction that breaks down organic matter, such as dirt, pollutants, or organic compounds[4]. This breakdown helps in the self-cleaning process, as the debris is gradually decomposed and removed from the surface. Its hydrophilic nature, which means it shows affinity to water, encourages water to spread into a thin layer rather than producing droplets. This effect serves to transport dirt particles away from the surface and prevents them from clinging tightly to it, making it simpler for rain or water to clean the coated glass surface[5]. Also, because silicon dioxide is a transparent substance, it may preserve the transparency of the glass surface allowing maximum light to pass through it as maximizing light transmission is critical for photovoltaic module performance[6].

2.1.3. ZrO₂

Zirconium Dioxide is mostly used as dopant material or composited with TiO₂, and SiO₂ for improved Self-cleaning applications. It is observed that adding ZrO₂, enhances the photo-electronic, chemical properties and greater photo-induced hydrophilicity in comparison to TiO₂ due to an increase in the surface hydroxyl groups that hence reducing electron hole recombination.[7][8].

2.1.4. Al₂O₃

Aluminum oxide is one of the most affordable materials with a wide range of uses. In recent years, there has been a lot of interest in using Al₂O₃ in coatings because of its antibacterial qualities, superior mechanical, electrical insulation, and high-temperature capabilities, and excellently impact, abrasion, and resistance to chemicals[9]. With high transparency, and superhydrophobic nature, Al₂O₃ is frequently applied on glass substrates used in for self-cleaning applications in PV modules[10].

2.1.5. ZnO

Zinc oxide is an essential semiconductor that is frequently used as a doped material due to its substantial excitation binding energy of 60 meV, broad band gap of 3.37 eV, low cost, nontoxicity, and optical and photochemical characteristics. In both basic and acidic conditions, ZnO surfaces outperform other photocatalytic surfaces in the breakdown of organic contaminants. ZnO also happens to be bio-safe and biocompatible, making it an ecologically friendly coating[11]. Zinc oxide has received substantial research due to its intriguing uses such as ZnO nanostructures in various morphologies, such as nanotubes, nanowires, nanoflowers, nanorods, and nanosheets have been synthesized utilizing physical and chemical techniques for self-cleaning applications in PV modules[12].

2.1.6. Polymer Coatings

There are numerous well-known hydrophobic polymers that have been employed in the creation of self-cleaning coatings, including polymethylmethacrylate (PMMA), polydimethylsiloxane (PDMS), and polytetrafluoroethylene (PTFE). Because of its low refractive index, hydrophobic PDMS polymer has been extensively accepted for self-cleaning coating, providing great transparency above 85% to the coated glass in the UV-vis region. Because the identical methyl groups of the PDMS polymer function as a binder, the hydrophobic PDMS polymer also provides excellent adherence to glass surfaces[13].

2.2. Performance of Self-Cleaning Materials

The performance of cleaning materials is usually tested in indoor and outdoor soiling conditions. The extended literature review for that is given below.

2.2.1. TiO₂

As discussed earlier in section 2.1.1., TiO₂ is known for its photo-induced superhydrophilicity which helps in photodegradation of organic contaminants and aid in washing away these contaminants by the action of water and gravity. But having the limitation of losing its self-cleaning property with time, it has been modified by compositing it with other metal-oxides to overcome the issue. Kenan and coworkers tested TiO₂ coatings at 45° in outdoor conditions for six months. The coating showed 31% of the degradation of WCA[14]. In 2022, Ajay and team studied TiO₂ nano colloidal solution thin films on glass substrate applied via dip-coating and obtained a WCA of 29°[15]. In another study, Narendra et al. obtained quantum sized TiO₂ nanoparticles using ethylene glycol by solvothermal route and spray coated them on glass substrate. He observed that films become super hydrophilic with WCA of 4.6°[16]. Jesus et al. investigated the WCA of TiO₂ coating deposited on LIFG substrate, one side by electron beam evaporation and the other by dip coating and found a low WCA of 0° indicating superhydrophilicity[17]. More studies on TiO₂ coatings showed that when coatings were prepared modified using fluorine free organic silane octadecyltrichlorosilane (OTS), they showed excellent self-cleaning ability against dust after washing with water[18]. In another interesting approach, bamboo timber was used as substrate for TiO₂ coatings with fluoroalkylsilane and showed a remarkable self-cleaning effect with having a hydrophobic nature (WCA=163°)[19].

2.2.2. Modified TiO₂

ODTS modified TiO₂ films deposited on glass substrate via sol-gel dip coating technique and showed improved WCA of 146° indicating superhydrophobicity[20]. Kokare et al. [14] employed ODS-modified TiO₂ nanoparticles to produce hydrophobic coating on glass substrates using a simple sol-gel and dip coating process with a WCA greater than 150°. The produced coatings were resistant to water jet

impact and repellent to colored and dirty water; yet the coatings remained opaque with a thickly white color [21].

2.2.3. SiO₂

SiO₂ coatings have also been used as anti-soiling coatings in many studies. Experimental investigation of SiO₂ based coating dripped on glass substrates were found to have good cleaning effect with a WCA greater than 100° [22]. In 2017, Zhang et al. developed hydrophobic fibered network SiO₂ film on soot via CVD having WCA of 166°[23]. It was observed when silica is modified using HMDS using a single step sol-gel process and applied over glass substrate via dip coating, the self-cleaning characteristic of the prepared coating showed enhancement in hydrophobic nature with WCA of 155°[24]. In a similar approach, one step spray coating of modified SiO₂ nanoparticles with Trimethoxypropylsilane (PTMS) upscaled the WCA to 152° [25]. The low-cost sol-gel dip-coating process was used to create coatings with good transmittance and exceptional superhydrophobicity. The base-catalyzed hydrolysis of tetraethyl orthosilicate and trimethylethoxysilane as co-precursors results in the creation of a hybrid sol containing methyl-enriched silica nanoparticles. The maximum transmittance is between 97.1% and 98.8%, with a water contact angle of up to 152°[26]. The substrate's coating layer was applied, increasing the transmittance to 99.6% at 600 nm. Atomic force microscopy (AFM) and scanning electron microscopy (SEM) observations of the coated layer's graded index and induced porous nature led to superhydrophilic behavior with a water contact angle that was close to 0°. The coating's super-hydrophilicity and self-cleaning abilities imply an improvement in the efficiency of solar PV modules[27]. A numerical analysis of SiO₂ based coatings showed an improved photoconversion efficiency of 26.5% from 25% and anti-dust properties with a WCA of 1.5°[28].

2.2.4. SiO₂-TiO₂

Anatase titanium dioxide (TiO₂)/silicon dioxide (SiO₂) nanocomposite coatings are among the permanent coatings that may effectively combine the super-hydrophilic characteristic of SiO₂ with the photocatalytic ability of anatase TiO₂[29]. SiO₂ and anatase TiO₂ may be formed using a variety of deposition techniques, however wet chemistry and multistep processes have largely been used to create anatase TiO₂/SiO₂ nanocomposite coatings[30]. Anatase TiO₂/SiO₂ nanocomposite coatings with multifunctional properties (anti-fogging, self-cleaning, and high optical transparency)

have been applied on polymer substrates utilising a low-temperature, atmospheric pressure PECVD process. The simultaneous production of anatase TiO_2 nanoparticles and their rapid subsequent deposition in an amorphous SiO_2 -like matrix were made possible by the atmospheric-pressure blown arc discharge torch. With WCA as low as 5° for the as deposited anatase $\text{TiO}_2/\text{SiO}_2$ nanocomposite coating made from the greatest HMDSO supply rate, the films' hydrophilicity was also improved[31]. We have created V- $\text{TiO}_2:\text{SiO}_2$ coatings that may be applied to solar glass covers over PV modules and simultaneously show antireflecting, self-cleaning, superhydrophilicity, and photocatalytic activity. The coating (15% V- $\text{TiO}_2:\text{SiO}_2$ thin film) has an optimized self-cleaning and antireflective property that results in an optical transmission that has a maximum transmission of 94.38% and an average transmission that is higher than that of bare glass with the smallest contact angle from 5° to 0° [32].

2.3. Synthesis and Fabrication of Anti-Soiling Coatings

The morphological, structural, and wettability of $\text{TiO}_2/\text{SiO}_2$ anti-soiling coatings have a significant impact on their performance. During the manufacturing process, multiple deposition processes can be used to adjust these characteristics. This section includes a thorough examination of the numerous deposition processes employed by researchers to create composite thin films, as well as their influence on the overall performance of self-cleaning.

2.3.1. Sol-Gel Route

The sol-gel technique is a flexible solution approach for fabricating inorganic coatings that includes the transition of a colloidal liquid 'sol' into a solid 'gel' phase. Sols and gels have enormous surface areas. Precursors for the 'sol' are often metal-organic compounds such as metal alkoxide/inorganic metal salts. The resulting 'gel' may be directly cast on surfaces and heated to form thin-film coatings. Surface chemical compositions, size, and morphologies of the films may be modified by modifying the precursor solution composition, utilizing the appropriate surfactant in the suitable concentration, and managing the amount of the hydrolysis and polycondensation processes[33]. However, this method's drawback is that it cannot be regulated. It is utilized with sub-applications like spin-coating and dip-coating as a result. Sol-gel form is affected by variables including chemicals, precursors, density, temperature, mixing ratios, surface material, forming method, and ranges of addition to the mixture[34].

2.3.1.1. Dip-Coating

In this method, because the material is dipped in this way, all sides of the surface are covered. When a heavier covering (like surface painting) can be applied, it is employed on those surfaces. According to this method's application is divided into 5 stages: immersion, start-up, deposition, evaporation, and drainage. Depending on the density and viscosity of the sol-gel, coating thickness may be adjusted by pulling out the material more quickly. Although it is a typical technique, it cannot be used on solar panels that are already installed and ready to go. A benefit of this approach is that both sides of the solar cover glass may be quickly and easily coated before manufacturing[35].

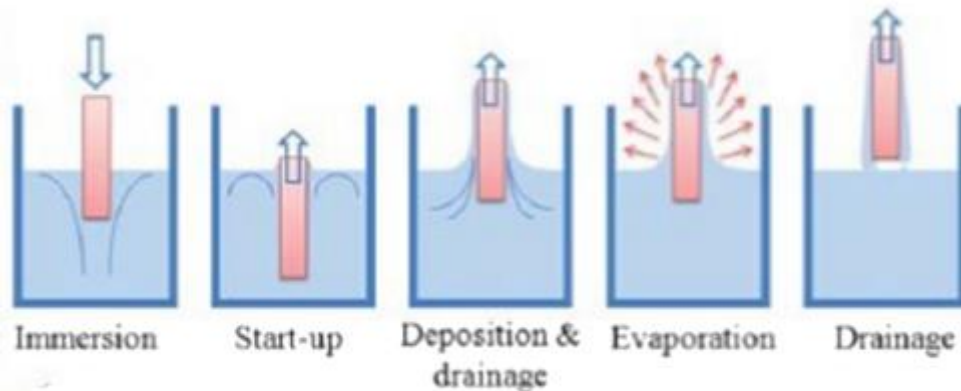


Figure 2.1. Schematic showing the process of Dip-coating[35]

Dip coating was employed to develop nano textured TiO_2 coatings. At a low dip-coating speed (6 mm/s) and a significant nitric acid content (0.5 M), films with good optical properties and high transmittance (1% loss in transmittance) may be achieved. Under optimal circumstances, low-temperature calcination (400°C) may even be sufficient to generate coatings with high functional qualities, making the technique suitable with some flexible substrates. High dip-coating rates, on the other hand, necessitate calcination at a higher temperature (500°C) to produce satisfactory film transmittance values[36]. Surface sol-gel process (SSP) is one of several modified procedures derived from the traditional sol-gel process that have been shown to be advantageous for the creation of super-wettable surfaces. SSP involves a nonaqueous condensation of metal-alkoxide precursor molecules and surface hydroxyl groups, followed by an aqueous hydrolysis of metal-alkoxide species that were adsorbed to create surface hydroxyl groups. This opens the way to produce a specified metal-

alkoxide coating onto a hydroxyl terminated surface. Tao et al. showed the manufacture of a self-cleaning anti-reflective coating by SSP, in which Silica coatings were changed with Titania by first adsorbing Titanium (IV) n-butoxide into silica coatings, followed by hydrolysis of the TiO_2 precursor in water and drying. titania was uniformly coated over SiO_2 and entered the nanopores between the silica nanoparticles, resulting in pore closure.[37]. The sol-gel dip coating, at a speed of 10cm/min, procedure was used to create very transparent thin films of TiO_2 - ZrO_2 - SiO_2 composites on glass, in which varied quantities of zirconia precursor were combined with titania precursor solution (0-20 mol% Zr with reference to Ti). A silica binder (27 mol% Si vs. Ti) was added to the alkoxide mixture to improve film adherence on glass[38]. To produce a cleaner surface on the glass covers of solar PV panels, a sol-gel based single component mixed silica coating formulation has been developed that concurrently exhibits antireflection and superhydrophobic characteristics. The water contact angle of approximately 150° needed for the coated surface to self-clean has been reached. Additionally, a significant transmission increase of almost 6% has been attained, allowing solar cells inside solar panels to receive the maximum amount of light for improved PV module output efficiency[39].

2.3.1.2. Spin Coating

Spin coating is a popular method for creating inexpensive thin coatings of organic and metal oxides. It entails the fast spinning of a liquid precursor or solution after it has been deposited onto a substrate to disperse the substance uniformly. The solvent also helped to evaporate throughout the spinning process, leaving behind a thin, homogeneous layer[40].

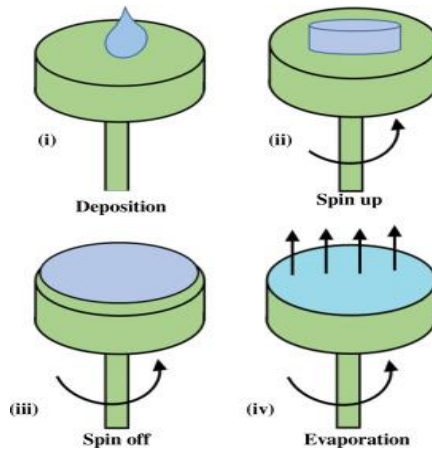


Figure 2.2. Graphical Illustration of spin coating[40]

Mihoreanu et al. presented silica-based thin films for self-cleaning uses in solar energy converters[41]. The coatings showed excellent hydrophilicity and enhanced photocatalytic activity when composited with TiO_2 . It was discovered that TiO_2 's bandgap was lowered from 3.05 to 2.74 eV, that the rate of electron-hole pair recombination was decreased, and that it had wonderful Superhydrophilic and self-cleaning properties within 30 minutes. About 75% of the exceptionally transparent coatings were created using a straightforward spin coating procedure[42]. Cedillo-González et al. investigated the resilience of thin films coated with TiO_2 in an acid rain-like environment. They created thick and mesoporous TiO_2 thin films for their investigation. Their findings demonstrated that thicker TiO_2 thin films outlasted their mesoporous counterparts in terms of durability[43].

2.3.1.3. Spray Coating

Spray coating is a well-known method for painting the car's bodies. The liquid coating substance is sprayed on the substrate surface by a machine that applies the coating. The liquid is atomized at the spray front head's nozzle, where a steady stream of spray droplets is produced. The liquid is broken down into tiny spraying droplets at the nozzle due to the system's entire air pressure. The wetting behavior, surface characteristics, distance between spray nozzles, coating speed, droplet size, and number of sprayed layers all affect coating quality[44].

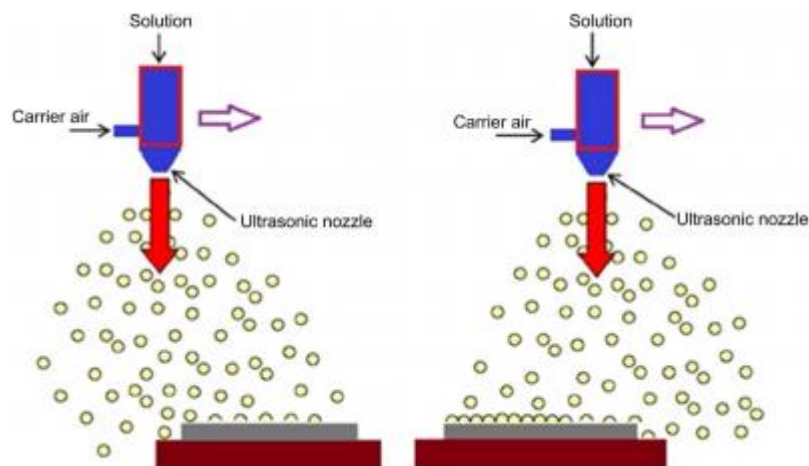


Figure 2.3. Schematics of spray coating method[44]

Mansur et al. studied the effect of adding silica into N doped titania of self-cleaning activity. Thin films' hydrophilic properties and visible light photocatalytic performance were both decreased by the addition of SiO₂, and as a result, their photocatalytic activity was comparable to that of an undoped TiO₂ thin film that had been calcined at 500°C. variables include a high band gap energy, small crystallite size, and low crystallinity and unwanted fracture patterns can be the root causes of this behavior[45]. Sol-gel technique was used to create TiO₂-SiO₂ composite films on glass substrates for self-cleaning applications. The impact of the coating cycle, calcined temperature, and SiO₂ concentration on the characteristics of TiO₂ thin film were discussed in this work. In comparison to 400 and 450 °C treated films, 500 °C treated films had higher optical and self-cleaning capabilities. The self-cleaning ability of the TiO₂ film decreased as the coating cycle and SiO₂ concentration were increased. The best material for TiO₂-SiO₂ composite films with greater self-cleaning properties had a single layer of 0.3 mol/L SiO₂ that was calcined at 500 °C and had a water contact angle of less than 3°[46]. In another study, Zr-modified TiO₂-SiO₂ coatings were developed. Over a 20-month outside exposure period, the outdoor performance of glass samples with float, commercial self-cleaning, and sol coating was rigorously examined. When discussing the potential applications of innovative materials, the impact of final installation orientation should not be disregarded. It was observed that the tilt angle has a considerable effect on the self-cleaning behavior[47]. Electrospinning was used to create self-cleaning TiO₂ coatings on glass substrate. The coating exhibited excellent superhydrophilic nature with WCA approximately equal to

2° and transparency > 90%[48]. Abdillah et al. studied the effect of electrospinning solution parameters on the morphology of TiO₂-SiO₂ nanofibers and concluded that with lower viscosity of the solution, beads on fiber morphology will appear and with increasing the voltage, the diameter reduces [49]. Porous SiO₂ anti-reflective coatings were developed using electrospinning technique on large area substrate by Raut et al. for solar cell application. Him and the team came up with a highly anti-reflective coatings having transmittance above 90% [50].

2.4. Performance Studies in Outdoor Conditions

Mostly nano-crystalline anatase/rutile titania (TiO₂) anchored with silica (SiO₂) nano-bridges make up the metal oxide combination in SurfaShield G. It is applied to glass surfaces using a straightforward air-sprayer and does not require any heat processing to provide adequate adherence to glass. The coated PV panels showed an average increase of 5-6% during the observed length of time under outside actual circumstances. The gain (P_m) was greatly boosted under diffuse lighting circumstances (up to 19%) and under irradiation with a high incidence angle (up to 30%), which was explained by the coating's antireflective qualities and the decreased deposition of dust on the glass surface[51]. Excellent anti-reflective, superhydrophilic, and photocatalytic capabilities were displayed TiO₂/SiO₂ coated films. The long-term outdoor experiment showed that the decrease of dust buildup on the panel surface caused a considerable rise in the power differential per day (P). P rose to its maximum level of 14.22% in dispersed light (on a foggy day), which may be due to the coating's antireflective qualities. The power output of the coated panels was 6.62% more than that of the uncoated panels while full time[52]. A mirror surface's adhesive force was significantly reduced by the engineering surface roughness associated with superwetting, leading to an intrinsic repulsion of inorganic soil and dust particles and an improvement in self-cleaning behavior owing to simple water layer sliding. In outdoor field testing, the superhydrophilic coating demonstrated an improvement in AS performance of 2.5 when compared to superhydrophobic coatings. To lessen organic dust cementation soiling on the mirror surface, superhydrophilicity was more successful[53]. Lanthanum phosphate modifies titania/silica coatings were also studied for self-cleaning applications. The dip coated samples showed almost 15%

reduction increase in the output voltage of solar panel module under outdoor exposure[54].

2.5. Performance Studies in Indoor Conditions

In a photovoltaic system, soiling primarily has the effect of reducing the amount of solar radiation that reaches the cell and, as a result, the amount of power produced. Although not the sole effect, this is the primary one. Other unfavorable impacts of soiling include the potential for the emergence of hot spots because of the dust's shading effect on areas of the module, which might lead to long-term deterioration aided by the cementation of the dust. The origins and effects of soiling have been examined in a variety of publications. Due to the numerous variables that affect deposition and the pressures that bind particles to the PV module's front sheet, soiling on PV modules is a complicated issue[55]. The significant heterogeneity of these parameters, which can be connected to the dust, the module, and the surroundings, was noted by Ilse et al. The particle size parameter appears to be one of the most important aspects in many studies, and PM2.5 and PM10 (airborne particles having a diameter smaller than or equal to 2.5 mm and 10 mm, respectively) are the main contributors to the modules' surface being covered[56], [57], [58]. The PV modules may become covered in an accumulation of all these impurities as well as the dust that is present at the PV plant site. Particle adhesion is caused by a few forces, including Van der Waals, capillary, gravitational, and electrostatic forces[59], [60]. Both the sources of the dust and the placement of the modules are crucial because they will affect the makeup of the dust and, as a result, the bonding, cementation, caking, and capillary phenomena. Numerous studies show a relationship between the pace of soiling and the kind of the dust[61], [62]. Dew may form on the modules depending on humidity and temperature, and just a single layer of water will strengthen the adhesion forces that cause the particles to cement together. Studies on indoor soiling must also take this element into consideration. Understanding these variables could help develop some soiling loss prediction models [63]. Its features also affect particle adhesion at the module size, particularly in relation to the glass surface. Some glass makers have been working on creating unique anti-soiling coatings for a while now to lessen the issue[64].

In a study by Miguel et al. the dust load varied from 1.30 to 1.63 g/m² and depending on the conditions under which it was deposited, electrical losses ranged from 4.73 to 6.90%[65]. According to Pedersen et al. the efficiency loss throughout the 2-month

test period was in the range of 0.2-0.3%. Based on gearbox losses of 1-2%, this figure was approximated[66]. Under sunlight, quantumized TiO₂ nanoparticles display strong photoinduced superhydrophilicity and photocatalytic activity. The anti-soiling coating on the minimodule was successfully created, and the coated module showed 2.5% less soiling loss than the uncoated substrate. The coating can be a way to lessen the loss from soiling[16].

In this investigation, we focus on SiO₂ modified TiO₂ thin films developed by sol-gel electrospinning and test them in a homemade indoor soiling chamber. The technique will deposit thin films having nanofibrous morphology of TiO₂/SiO₂ on glass substrates. It is an emerging technique for developing anti-soiling coatings for PV modules. The primary motivation for choosing this technique is that it can be used for large-area applications, doesn't require costly vacuum chambers, and multiple glass substrates can be mounted on the collector plate at a time for deposition which can help in reducing solution wastage. Although TiO₂/SiO₂ thin films have been widely studied but very scarce data is available on electro spun TiO₂/SiO₂ composite thin films with respect to their self-cleaning application in solar cells and how it will change under soiling when tilt angle is varied. Therefore, the purpose of this study is to synthesize TiO₂/SiO₂ thin films on glass substrates and explore their anti-soiling property by testing in an indoor soiling station.

Summary

TiO₂ and SiO₂ coatings are the main topics of this chapter's investigation into the world of self-cleaning materials. The capacity of TiO₂ coatings to eliminate organic pollutants via photo-induced superhydrophilicity has been thoroughly investigated. But over time, their self-cleaning property gets worse. To combat this, scientists have investigated how TiO₂ may be altered by mixing it with other metal oxides, producing better water contact angles and self-cleaning properties. As anti-soiling coatings, SiO₂ coatings have also demonstrated promise. These coatings have been made using a variety of deposition processes, including spray coating, spin coating, and sol-gel dip coating, each of which affects the coatings' morphological, structural, and wettability characteristics. The efficiency of these coatings in terms of self-cleaning, superhydrophilicity, and improved transmittance has been confirmed by outdoor

performance studies. The long-term objective of this research is to create resilient and effective self-cleaning components appropriate for a variety of applications, including solar panels.

References

- [1] V. Zharvan, R. Daniyati, A. S. Nur Ichzan, G. Yudoyono, and Darminto, “Study on fabrication of TiO₂ thin films by spin-coating and their optical properties,” in *AIP Conference Proceedings*, American Institute of Physics Inc., Mar. 2016. doi: 10.1063/1.4943713.
- [2] M. A. M. L. de Jesus, G. Timò, C. Agustín-Sáenz, I. Braceras, M. Cornelli, and A. de M. Ferreira, “Anti-soiling coatings for solar cell cover glass: Climate and surface properties influence,” *Solar Energy Materials and Solar Cells*, vol. 185, pp. 517–523, Oct. 2018, doi: 10.1016/j.solmat.2018.05.036.
- [3] R. J. Isaifan *et al.*, “Improved Self-cleaning Properties of an Efficient and Easy to Scale up TiO₂ Thin Films Prepared by Adsorptive Self-Assembly,” *Sci Rep*, vol. 7, no. 1, pp. 1–9, 2017, doi: 10.1038/s41598-017-07826-0.
- [4] C. Tao *et al.*, “Fabrication of robust, self-cleaning, broadband TiO₂–SiO₂ double-layer antireflective coatings with closed-pore structure through a surface sol-gel process,” *J Alloys Compd*, vol. 747, pp. 43–49, May 2018, doi: 10.1016/j.jallcom.2018.03.008.
- [5] W. Zhao and H. Lu, “Self-cleaning performance of super-hydrophilic coatings for dust deposition reduction on solar photovoltaic cells,” *Coatings*, vol. 11, no. 9, Sep. 2021, doi: 10.3390/coatings11091059.
- [6] J. J. Wang, D. S. Wang, J. Wang, W. L. Zhao, and C. W. Wang, “High transmittance and superhydrophilicity of porous TiO₂/SiO₂ bi-layer films without UV irradiation,” *Surf Coat Technol*, vol. 205, no. 12, pp. 3596–3599, Mar. 2011, doi: 10.1016/j.surfcoat.2010.12.033.
- [7] S. M. Simon *et al.*, “Robust polymer incorporated TiO₂-ZrO₂ microsphere coatings by electrospraying technique with excellent and durable self cleaning, antibacterial and photocatalytic functionalities,” *J Appl Polym Sci*, vol. 138, no. 34, Sep. 2021, doi: 10.1002/app.50880.
- [8] S. M. Simon *et al.*, “Morphological and thermal studies of mesoporous TiO₂-ZrO₂ and TiO₂-ZrO₂-polymer composites as potential self cleaning surface,” in *Materials Today: Proceedings*, Elsevier Ltd, 2019, pp. 1327–1332. doi: 10.1016/j.matpr.2020.04.181.

- [9] R. S. Sutar *et al.*, “Superhydrophobic Al_2O_3 –polymer composite coating for self-cleaning applications,” *Coatings*, vol. 11, no. 10, Oct. 2021, doi: 10.3390/coatings11101162.
- [10] S. Sutha, S. Suresh, B. Raj, and K. R. Ravi, “Transparent alumina based superhydrophobic self-cleaning coatings for solar cell cover glass applications,” *Solar Energy Materials and Solar Cells*, vol. 165, pp. 128–137, Jun. 2017, doi: 10.1016/j.solmat.2017.02.027.
- [11] B. Stieberova *et al.*, “Application of ZnO Nanoparticles in a Self-cleaning Coating on a Metal Panel: An Assessment of Environmental Benefits,” *ACS Sustain Chem Eng*, vol. 5, no. 3, pp. 2493–2500, Mar. 2017, doi: 10.1021/acssuschemeng.6b02848.
- [12] S. Nundy, A. Ghosh, and T. K. Mallick, “Hydrophilic and Superhydrophilic Self-Cleaning Coatings by Morphologically Varying ZnO Microstructures for Photovoltaic and Glazing Applications,” *ACS Omega*, vol. 5, no. 2, pp. 1033–1039, Jan. 2020, doi: 10.1021/acsomega.9b02758.
- [13] A. Syafiq *et al.*, “Application of transparent self-cleaning coating for photovoltaic panel: a review,” *Current Opinion in Chemical Engineering*, vol. 36. Elsevier Ltd, Jun. 01, 2022. doi: 10.1016/j.coche.2022.100801.
- [14] IEEE Electron Devices Society, IEEE Photonics Society, Institute of Electrical and Electronics Engineers, H. IEEE Photovoltaic Specialists Conference (45th : 2018 : Waikoloa, H. Kōki Denryoku Kōka no Kiso to Ōyō ni kansuru Shinpojūmu (28th : 2018 : Waikoloa, and H. European Photovoltaic Solar Energy Conference (34th : 2018 : Waikoloa, *2018 IEEE 7th World Conference on Photovoltaic Energy Conversion (WCPEC) (A Joint Conference of 45th IEEE PVSC, 28th PVSEC & 34th EU PVSEC) : 10-15 June 2018*.
- [15] A. Kumar, V. K. Saxena, R. Thangavel, and B. K. Nandi, “A dual effect of surface roughness and photocatalysis of crystalline TiO_2 -thin film for self-cleaning application on a photovoltaic covering glass,” *Mater Chem Phys*, vol. 289, Sep. 2022, doi: 10.1016/j.matchemphys.2022.126427.
- [16] N. Chundi, E. Ramasamy, S. Koppoju, S. Mallick, A. Kottantharayil, and S. Sakthivel, “Quantum-sized TiO_2 particles as highly stable super-hydrophilic and self-cleaning

- antisoiling coating for photovoltaic application,” *Solar Energy*, vol. 258, pp. 194–202, Jul. 2023, doi: 10.1016/j.solener.2023.04.062.
- [17] M. A. M. L. de Jesus, G. Timò, C. Agustín-Sáenz, I. Braceras, M. Cornelli, and A. de M. Ferreira, “Anti-soiling coatings for solar cell cover glass: Climate and surface properties influence,” *Solar Energy Materials and Solar Cells*, vol. 185, pp. 517–523, Oct. 2018, doi: 10.1016/j.solmat.2018.05.036.
- [18] N. Pratiwi, Zulhadjri, S. Arief, Admi, and D. V. Wellia, “Self-cleaning material based on superhydrophobic coatings through an environmentally friendly sol–gel method,” *J Solgel Sci Technol*, vol. 96, no. 3, pp. 669–678, Dec. 2020, doi: 10.1007/s10971-020-05389-7.
- [19] J. Li *et al.*, “Durable, self-cleaning and superhydrophobic bamboo timber surfaces based on TiO₂ films combined with fluoroalkylsilane,” *Ceram Int*, vol. 42, no. 8, pp. 9621–9629, Jun. 2016, doi: 10.1016/j.ceramint.2016.03.047.
- [20] N. Pratiwi, Zulhadjri, S. Arief, and D. V. Wellia, “A Facile Preparation of Transparent Ultrahydrophobic Glass via TiO₂/Octadecyltrichlorosilane (ODTS) Coatings for Self-Cleaning Material,” *ChemistrySelect*, vol. 5, no. 4, pp. 1450–1454, Jan. 2020, doi: 10.1002/slct.201904153.
- [21] A. M. Kokare, R. S. Sutar, S. G. Deshmukh, R. Xing, S. Liu, and S. S. Latthe, “ODS-Modified TiO₂ nanoparticles for the preparation of self-cleaning superhydrophobic coating,” in *AIP Conference Proceedings*, American Institute of Physics Inc., May 2018. doi: 10.1063/1.5033004.
- [22] Y. Y. Quan and L. Z. Zhang, “Experimental investigation of the anti-dust effect of transparent hydrophobic coatings applied for solar cell covering glass,” *Solar Energy Materials and Solar Cells*, vol. 160, pp. 382–389, Feb. 2017, doi: 10.1016/j.solmat.2016.10.043.
- [23] F. Zhang *et al.*, “Fabrication of transparent superhydrophobic glass with fibered-silica network,” *Appl Surf Sci*, vol. 407, pp. 526–531, Jun. 2017, doi: 10.1016/j.apsusc.2017.02.207.
- [24] K. Alam *et al.*, “Development of Anti-Reflective and Self-Cleaning SiO₂Nanoparticles Coatings for Photovoltaic Panels,” in *1st International Conference on Electrical*,

Communication and Computer Engineering, ICECCE 2019, Institute of Electrical and Electronics Engineers Inc., Jul. 2019. doi: 10.1109/ICECCE47252.2019.8940647.

- [25] N. Pratiwi, Zulhadjri, S. Arief, Admi, and D. V. Wellia, “Self-cleaning material based on superhydrophobic coatings through an environmentally friendly sol–gel method,” *J Solgel Sci Technol*, vol. 96, no. 3, pp. 669–678, Dec. 2020, doi: 10.1007/s10971-020-05389-7.
- [26] J. Xu *et al.*, “Superhydrophobic silica antireflective coatings with high transmittance via one-step sol-gel process,” *Thin Solid Films*, vol. 631, pp. 193–199, Jun. 2017, doi: 10.1016/j.tsf.2017.03.005.
- [27] K. Alam *et al.*, “Antireflection, superhydrophilic nano-porous SiO₂ coating based on aerosol impact spray deposition technique for solar PV module,” *Coatings*, vol. 9, no. 8, Aug. 2019, doi: 10.3390/coatings9080497.
- [28] M. I. Hossain, B. Aïssa, A. Samara, S. A. Mansour, C. A. Broussillou, and V. B. Benito, “Hydrophilic Antireflection and Antidust Silica Coatings,” *ACS Omega*, vol. 6, no. 8, pp. 5276–5286, Mar. 2021, doi: 10.1021/acsomega.0c05405.
- [29] F. Liu, J. Shen, W. Zhou, S. Zhang, and L. Wan, “In situ growth of TiO₂/SiO₂ nanospheres on glass substrates via solution impregnation for antifogging,” *RSC Adv*, vol. 7, no. 26, pp. 15992–15996, 2017, doi: 10.1039/c6ra27276b.
- [30] N. Saxena, T. Naik, and S. Paria, “Organization of SiO₂ and TiO₂ Nanoparticles into Fractal Patterns on Glass Surface for the Generation of Superhydrophilicity,” *Journal of Physical Chemistry C*, vol. 121, no. 4, pp. 2428–2436, Feb. 2017, doi: 10.1021/acs.jpcc.6b09519.
- [31] J. B. Chemin *et al.*, “Transparent anti-fogging and self-cleaning TiO₂/SiO₂ thin films on polymer substrates using atmospheric plasma,” *Sci Rep*, vol. 8, no. 1, Dec. 2018, doi: 10.1038/s41598-018-27526-7.
- [32] D. Adak *et al.*, “Self-cleaning V-TiO₂:SiO₂ thin-film coatings with enhanced transmission for solar glass cover and related applications,” *Solar Energy*, vol. 155, pp. 410–418, 2017, doi: 10.1016/j.solener.2017.06.014.

- [33] N. T. Padmanabhan and H. John, "Titanium dioxide based self-cleaning smart surfaces: A short review," *Journal of Environmental Chemical Engineering*, vol. 8, no. 5. Elsevier Ltd, Oct. 01, 2020. doi: 10.1016/j.jece.2020.104211.
- [34] S. Bashir Khan, H. Wu, C. Pan, and Z. Zhang, "A Mini Review: Antireflective Coatings Processing Techniques, Applications and Future Perspective," *Research & Reviews: Journal of Material Sciences*, vol. 05, no. 06, 2017, doi: 10.4172/2321-6212.1000192.
- [35] A. S. Sarkın, N. Ekren, and Ş. Sağlam, "A review of anti-reflection and self-cleaning coatings on photovoltaic panels," *Solar Energy*, vol. 199. Elsevier Ltd, pp. 63–73, Mar. 15, 2020. doi: 10.1016/j.solener.2020.01.084.
- [36] M. G. Salvaggio *et al.*, "Functional nano-textured titania-coatings with self-cleaning and antireflective properties for photovoltaic surfaces," *Solar Energy*, vol. 125, pp. 227–242, Feb. 2016, doi: 10.1016/j.solener.2015.12.012.
- [37] C. Tao *et al.*, "Fabrication of robust, self-cleaning, broadband TiO₂–SiO₂ double-layer antireflective coatings with closed-pore structure through a surface sol-gel process," *J Alloys Compd*, vol. 747, pp. 43–49, May 2018, doi: 10.1016/j.jallcom.2018.03.008.
- [38] N. Vodišek, K. Ramanujachary, V. Brezová, and U. Lavrenčič Štangar, "Transparent titania-zirconia-silica thin films for self-cleaning and photocatalytic applications," *Catal Today*, vol. 287, pp. 142–147, Jun. 2017, doi: 10.1016/j.cattod.2016.12.026.
- [39] D. Adak, R. Bhattacharyya, H. Saha, and P. S. Maiti, "Sol-gel processed silica based highly transparent self-cleaning coatings for solar glass covers," in *Materials Today: Proceedings*, Elsevier Ltd, 2019, pp. 2429–2433. doi: 10.1016/j.matpr.2020.01.331.
- [40] B. S. Yilbas, A. Al-Sharafi, and H. Ali, "Surfaces for Self-Cleaning," in *Self-Cleaning of Surfaces and Water Droplet Mobility*, Elsevier, 2019, pp. 45–98. doi: 10.1016/b978-0-12-814776-4.00003-3.
- [41] C. Mihoreanu, A. Banciu, A. Enesca, and A. Duta, "Silica-Based Thin Films for Self-Cleaning Applications in Solar Energy Converters," *Journal of Energy Engineering*, vol. 143, no. 5, Oct. 2017, doi: 10.1061/(asce)ey.1943-7897.0000461.
- [42] S. Prabhu, L. Cindrella, O. Joong Kwon, and K. Mohanraju, "Superhydrophilic and self-cleaning rGO-TiO₂ composite coatings for indoor and outdoor photovoltaic

- applications,” *Solar Energy Materials and Solar Cells*, vol. 169, pp. 304–312, Sep. 2017, doi: 10.1016/j.solmat.2017.05.023.
- [43] E. I. Cedillo-González *et al.*, “Influence of domestic and environmental weathering in the self-cleaning performance and durability of TiO₂ photocatalytic coatings,” *Build Environ*, vol. 132, pp. 96–103, Mar. 2018, doi: 10.1016/j.buildenv.2018.01.028.
- [44] A. Mishra, N. Bhatt, and A. K. Bajpai, “Nanostructured superhydrophobic coatings for solar panel applications,” in *Nanomaterials-Based Coatings: Fundamentals and Applications*, Elsevier, 2019, pp. 397–42. doi: 10.1016/B978-0-12-815884-5.00012-0.
- [45] M. Momeni, H. Saghafian, F. Golestani-Fard, N. Barati, and A. Khanahmadi, “Effect of SiO₂ addition on photocatalytic activity, water contact angle and mechanical stability of visible light activated TiO₂ thin films applied on stainless steel by a sol gel method,” *Appl Surf Sci*, vol. 392, pp. 80–87, Jan. 2017, doi: 10.1016/j.apsusc.2016.08.165.
- [46] M. Zhang, L. E. R. Zhang, and Z. Liu, “The effect of SiO₂ on TiO₂-SiO₂ composite film for self-cleaning application,” *Surfaces and Interfaces*, vol. 16, pp. 194–198, Sep. 2019, doi: 10.1016/j.surfin.2018.10.005.
- [47] A. Šuligoj *et al.*, “Field test of self-cleaning Zr-modified-TiO₂-SiO₂ films on glass with a demonstration of their anti-fogging effect,” *Materials*, vol. 12, no. 13, Jul. 2019, doi: 10.3390/ma12132196.
- [48] V. A. Ganesh, A. S. Nair, H. K. Raut, T. M. Walsh, and S. Ramakrishna, “Photocatalytic superhydrophilic TiO₂ coating on glass by electrospinning,” *RSC Adv*, vol. 2, no. 5, pp. 2067–2072, Mar. 2012, doi: 10.1039/c2ra00921h.
- [49] U. Abdillah *et al.*, “The effect of various electrospinning parameter and sol-gel concentration on morphology of silica and titania nanofibers,” *IOP Conf Ser Mater Sci Eng*, vol. 1231, no. 1, p. 012012, Feb. 2022, doi: 10.1088/1757-899x/1231/1/012012.
- [50] H. K. Raut, A. S. Nair, S. S. Dinachali, V. A. Ganesh, T. M. Walsh, and S. Ramakrishna, “Porous SiO₂ anti-reflective coatings on large-area substrates by electrospinning and their application to solar modules,” *Solar Energy Materials and Solar Cells*, vol. 111, pp. 9–15, 2013, doi: 10.1016/j.solmat.2012.12.023.

- [51] I. Arabatzis *et al.*, “Photocatalytic, self-cleaning, antireflective coating for photovoltaic panels: Characterization and monitoring in real conditions,” *Solar Energy*, vol. 159, pp. 251–259, Jan. 2018, doi: 10.1016/j.solener.2017.10.088.
- [52] W. Thongsuwan, W. Sroila, T. Kumpika, E. Kantarak, and P. Singjai, “Antireflective, photocatalytic, and superhydrophilic coating prepared by facile sparking process for photovoltaic panels,” *Sci Rep*, vol. 12, no. 1, Dec. 2022, doi: 10.1038/s41598-022-05733-7.
- [53] G. G. Jang, D. B. Smith, G. Polizos, L. Collins, J. K. Keum, and D. F. Lee, “Transparent superhydrophilic and superhydrophobic nanoparticle textured coatings: Comparative study of anti-soiling performance,” *Nanoscale Adv*, vol. 1, no. 3, pp. 1249–1260, 2019, doi: 10.1039/c8na00349a.
- [54] V. S. Smitha, K. Vidya, M. Jayasankar, A. Peer Mohamed, U. S. Hareesh, and K. G. K. Warriar, “Energy revamping of solar panels through titania nanocomposite coatings; Influence of aqueous silica precursor,” *RSC Adv*, vol. 6, no. 37, pp. 31114–31121, 2016, doi: 10.1039/c6ra03581g.
- [55] L. Micheli and M. Muller, “An investigation of the key parameters for predicting PV soiling losses,” *Progress in Photovoltaics: Research and Applications*, vol. 25, no. 4, pp. 291–307, Apr. 2017, doi: 10.1002/pip.2860.
- [56] K. K. Ilse, B. W. Figgis, V. Naumann, C. Hagendorf, and J. Bagdahn, “Fundamentals of soiling processes on photovoltaic modules,” *Renewable and Sustainable Energy Reviews*, vol. 98, pp. 239–254, Dec. 2018, doi: 10.1016/j.rser.2018.09.015.
- [57] B. Figgis, A. Ennaoui, S. Ahzi, and Y. Rémond, “Review of PV soiling particle mechanics in desert environments,” *Renewable and Sustainable Energy Reviews*, vol. 76. Elsevier Ltd, pp. 872–881, 2017. doi: 10.1016/j.rser.2017.03.100.
- [58] K. Sun, L. Lu, Y. Jiang, Y. Wang, K. Zhou, and Z. He, “Integrated effects of PM_{2.5} deposition, module surface conditions and nanocoatings on solar PV surface glass transmittance,” *Renewable and Sustainable Energy Reviews*, vol. 82. Elsevier Ltd, pp. 4107–4120, Feb. 01, 2018. doi: 10.1016/j.rser.2017.10.062.
- [59] C. S. Jiang, H. R. Moutinho, B. To, C. Xiao, L. J. Simpson, and M. M. Al-Jassim, “Long-lasting strong electrostatic attraction and adhesion forces of dust particles on

- photovoltaic modules,” *Solar Energy Materials and Solar Cells*, vol. 204, Jan. 2020, doi: 10.1016/j.solmat.2019.110206.
- [60] H. R. Moutinho *et al.*, “Adhesion mechanisms on solar glass: Effects of relative humidity, surface roughness, and particle shape and size,” *Solar Energy Materials and Solar Cells*, vol. 172, pp. 145–153, Dec. 2017, doi: 10.1016/j.solmat.2017.07.026.
- [61] P. Ferrada *et al.*, “Physicochemical characterization of soiling from photovoltaic facilities in arid locations in the Atacama Desert,” *Solar Energy*, vol. 187, pp. 47–56, Jul. 2019, doi: 10.1016/j.solener.2019.05.034.
- [62] J. J. John, S. Warade, G. Tamizhmani, and A. Kottantharayil, “Study of soiling loss on photovoltaic modules with artificially deposited dust of different gravimetric densities and compositions collected from different locations in India,” *IEEE J Photovolt*, vol. 6, no. 1, pp. 236–243, Jan. 2016, doi: 10.1109/JPHOTOV.2015.2495208.
- [63] L. Micheli, M. G. Deceglie, and M. Muller, “Predicting photovoltaic soiling losses using environmental parameters: An update,” *Progress in Photovoltaics: Research and Applications*, vol. 27, no. 3, pp. 210–219, Mar. 2019, doi: 10.1002/pip.3079.
- [64] D. Goossens, “Wind tunnel protocol to study the effects of anti-soiling and anti-reflective coatings on deposition, removal, and accumulation of dust on photovoltaic surfaces and consequences for optical transmittance,” *Solar Energy*, vol. 163, pp. 131–139, Mar. 2018, doi: 10.1016/j.solener.2018.01.088.
- [65] M. Á. Muñoz-García, T. Fouris, and E. Pilat, “Analysis of the soiling effect under different conditions on different photovoltaic glasses and cells using an indoor soiling chamber,” *Renew Energy*, vol. 163, pp. 1560–1568, Jan. 2021, doi: 10.1016/j.renene.2020.10.027.
- [66] W. Oh *et al.*, “Evaluation of anti-soiling and anti-reflection coating for photovoltaic modules,” *J Nanosci Nanotechnol*, vol. 16, no. 10, pp. 10689–10692, Oct. 2016, doi: 10.1166/jnn.2016.13219.

Chapter: 3 Introduction to Deposition, Characterization and Anti-Soiling Testing

This chapter underlines an introduction of the thin film deposition and characterization techniques used to study optical, structural, morphological and Photovoltaic properties. Further, it also describes the working principle of these techniques.

3.1. Deposition

Various deposition methods have been used to deposit self-cleaning coatings on the glass substrates including sol-gel methods such as spin coating and dip coating, sputtering, PVD, and CVD. But these methods have their cons, as sol gel methods are volatile, so it is difficult to control the thickness of the coating. Sputtering is a batch process but is costly. Although the thickness can be controlled in PVD and CVD but both methods are expensive. Due to these aspects, electrospinning is used.

3.1.1. Electrospinning

Another straightforward chemical solution-based method for producing 1D nanostructures, specifically nanofibers with a very high surface area-to-volume ratio, is electrospinning. The primary component of this method is the use of a high voltage power source to inject the melt precursor through a syringe using an electrode made of metal. As a result, melt droplets are jetted (Taylor cone) in the direction of the collector (counter electrode), where they solidify into nanofibers and deposit them on the collection plate[1].

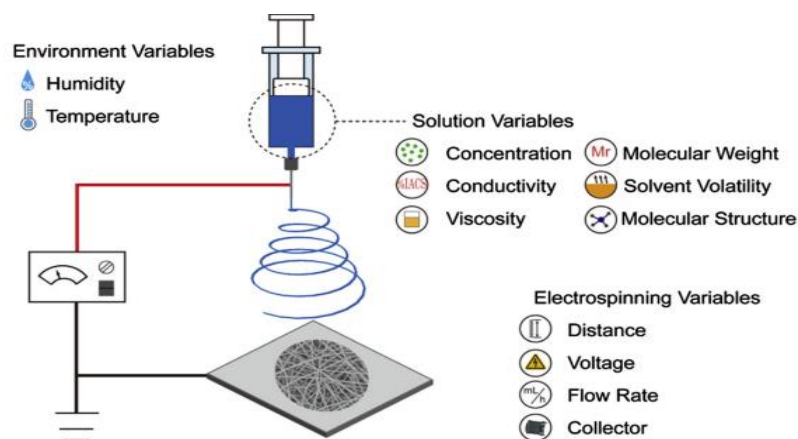


Figure 3.1. Schematic diagram of a conventional electrospinning setup[2]

Despite the simplicity and low cost of electrospinning, there are numerous processing variables that could have a significant impact on fiber production and nanostructure. The operational settings and processing conditions for an electrospinning procedure are shown in Fig. 3.1. The stabilization of electro spun ultrathin fibers requires optimized process parameters.

When a high voltage is applied during the electrospinning process, the polymer solution droplet at the needle tip deforms into a cone shape (sometimes referred to as a Taylor cone) because of electrostatic forces. The process of electrospinning has been thought to be started by a strong electrostatic force. The charged solution jet at the spinneret tip adjusts its size to preserve the balance of forces when subjected to a high electrostatic field. The induction charges on the surface reject one another and create shear stresses as the strength of the electrostatic field increases. These repelling forces occur in the opposite direction of surface tension, which causes the solution drop to extend into a Taylor cone and contributes to the beginning of the surface. The balance of repulsive forces fails when the electrostatic field reaches the critical voltage and as a result, a charged jet ejects from the conical drop's tip[2].

3.1.2. Plasma Cleaning

Prior to the deposition of thin films, the surface of the substrate is cleaned with plasma to remove very small organic and inorganic particles, oil, and other contaminants. Substrates typically have dust or organic residue on their surfaces, which makes them hydrophobic and difficult to spin coat with solution processable thin films. As a result,

during the deposition process, these surfaces are not entirely covered. To combat this, a cleaning method known as plasma cleaning is utilized to prepare the substrate surface for the deposition of the thin films by making it more hydrophilic, hence increasing the adhesion.

To clean the glass substrate surfaces of minute residual particles, substrates are inserted within the plasma cleaner. To establish a vacuum, the chamber is then sealed, and the vacuum pump is turned on to totally remove the air that was previously present. Then, to remove any contamination from the surface of the glass substrates, a mixture of oxygen and argon is injected within the chamber to produce a purple-colored plasma. Before the deposition of thin films, a plasma treatment of 10 to 20 minutes is typically advised.



Figure 3.2. Plasma Cleaning setup

3.2. Characterization

The coatings were characterized for their structural, optical, and morphological properties using the below mentioned techniques.

3.2.1. X-Ray Diffraction (XRD)

A non-destructive analytical method known as X-ray diffraction, or XRD, is used to examine the structural and crystallographic characteristics of samples made of powder and thin films. Additionally, it is utilized to examine the samples' crystallinity and crystal structure. Additionally, the sample's crystalline phases, concentration profiles, film thickness, and atomic patterns can all be determined using this method.

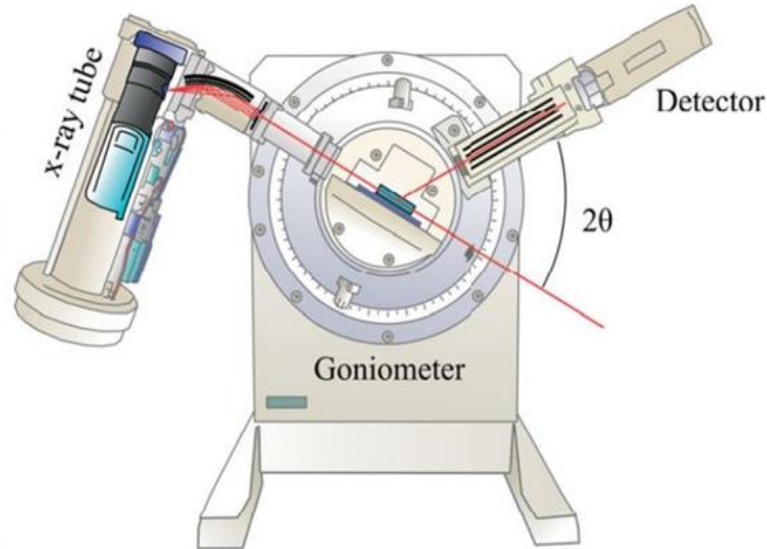


Figure 3.3. Schematic diagram of X-ray diffraction[3]

In XRD, a sample is exposed to a collimated beam of X-rays with a wavelength in the range of 0.5-2, which are then diffracted by the various crystalline phases according to the relationship $d = 2d \sin$ (Bragg's equation), where d is the interatomic spacing in the crystalline phase[3]. There are three primary components that make up XRD diffractometers:

- X-Ray tube
- Sample mounting stage
- X-Ray detector

Inside the X-Ray tubes, where an electron beam is created by heating a filament, X-rays are produced. Then, by using voltage, these electrons are hastened before being hit with a target material. After that, the target's inner shell electrons are dislodged by an electron beam with enough energy to do so, which results in the production of distinctive X-Rays. The specimen is then exposed to these X-Rays at an angle of 2° . The diffracted X-rays are recorded by an X-Ray detector, which is positioned at an angle of 2° . The sample mounting stage continually rotates in the path of the collimated X-Ray beam due to the diffractometer's design. Goniometer is the term used to describe the equipment that maintains the angle and rotates the sample mounting stage [4].

3.2.2. UV-VIS-NIR Spectroscopy

UV-Vis-NIR spectroscopy is an analytical tool which is used to study light spectrum response (absorbance, transmittance, and reflectance) of liquids and solid samples. It

has been frequently used to probe materials such as semiconductors, thin film coatings, glass etc. UV-Vis-NIR spectroscopy works on the principle of Beer Lambert's law which states that the absorbance of a solution directly proportional to the concentration of the absorbing material present in the solution [5].

The following equation expresses Beer Lambert's law:

$$A = \log \frac{I_0}{I} = \epsilon lc = \alpha l$$

Where "A" stands for optical density or absorbance, "I₀" for incident light intensity, "I" for transmitted light intensity, "ε" for molar extinction coefficient, "c" for solution sample concentration, and "α" for absorption coefficient. Additionally, transmittance is represented by the fraction $\frac{I_0}{I}$.

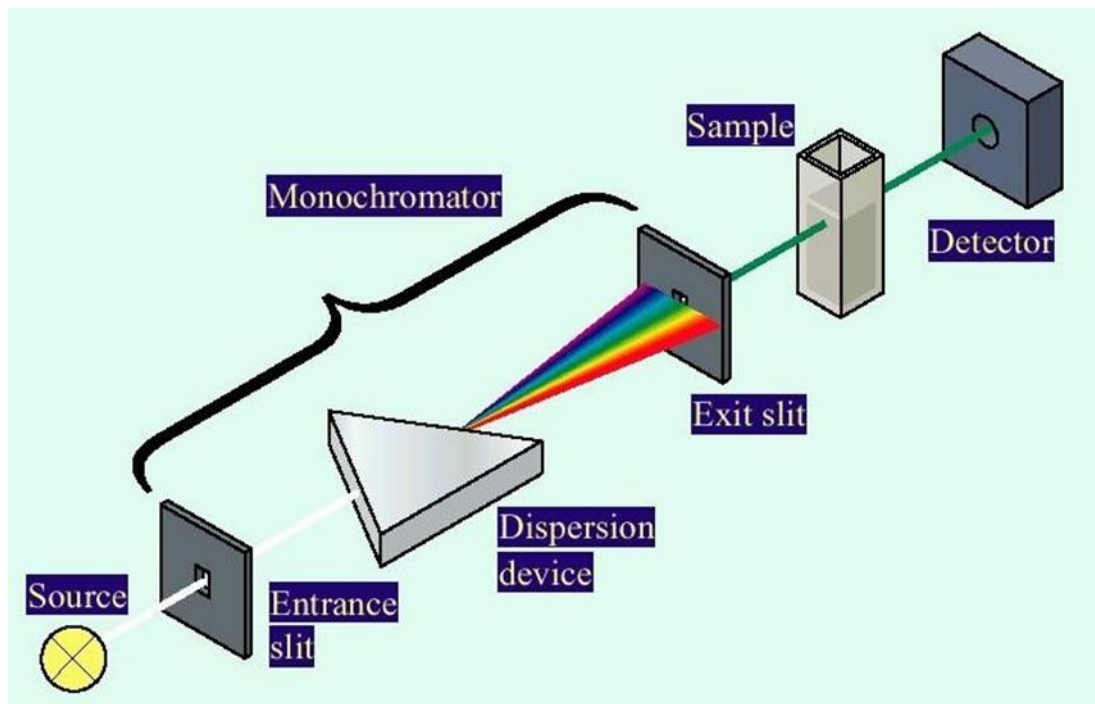


Figure 3.4. Schematics of UV-VIS-NIR spectroscopy[6]

In general, there are two types of UV-Vis-NIR spectrophotometers: single beam and double beam-based spectrophotometers. Figure 3.4 illustrates the four main parts of single beam UV-Vis-NIR spectrophotometers:

- light source
- Monochromator
- Sample

- Detector

The light source produces a continuous light beam as it enters the monochromator chamber. The process whereby the continuous light spectrum is divided into discrete photons based on various wavelengths. The monochromatic light is then shone on the sample, where it either absorbs, transmits, or is reflected. The response of the sample following its interaction with the laser beam is then measured against various wavelengths by the appropriate detectors [6].

3.2.3. Scanning electron Microscopy (SEM)

A non-destructive imaging method called scanning electron microscopy is used to examine or capture an image of a specimen under observation. It offers details about the sample's morphology, chemical composition, and surface texture. It has frequently been employed to investigate specimens made of solid powder or thin films.

In the SEM, the specimen is bombarded with a concentrated electron beam that is then raster scanned through a small rectangular area. Various types of events, including the emission of secondary electrons and photon emissions, happen when the focused beam of electrons interacts with the specimen's surface. The brightness of these electrons in a conventional cathode ray tube allows for an image to be formed based on this response, which can be effectively recorded on a detector. These images are identical to those produced by an optical microscope, but they have been magnified further and have a deeper nanoscale regime [7]. SEMs often include the following elements:

- Sample mounting stage
- Detectors, for all types of electrons or signals
- Display or output systems
- Electron source gun
- Electron lenses

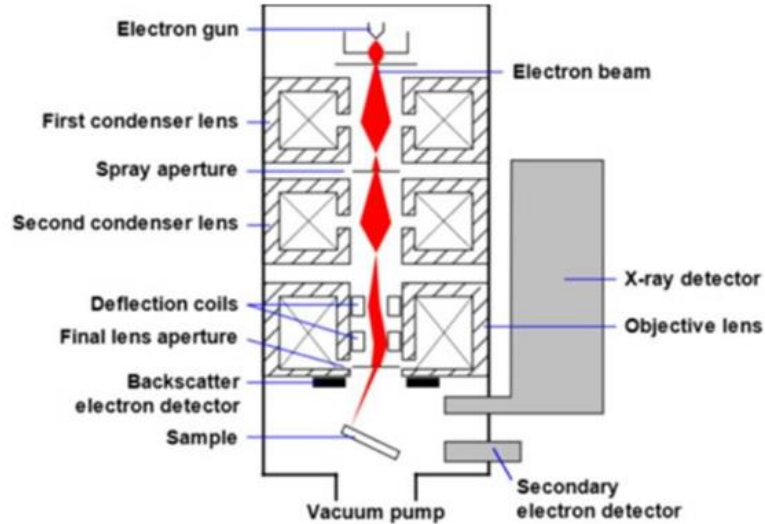


Figure 3.5. Schematic diagram of SEM [7]

3.2.4. Fourier Transform Infrared spectroscopy (FTIR)

Another analytical method to investigate the chemical interactions between different molecules in a sample of liquid or solid matter is Fourier transform infrared spectroscopy (FTIR). The dopant interactions with the perovskite precursors have been extensively studied using FTIR in perovskite-based photovoltaics. Additionally, it has been extensively used in analytical chemistry to detect the presence of different functional groups.

The fundamentals of FTIR are the same as those of UV-vis spectroscopy, with the exception that FTIR uses infrared light to probe the sample being observed. Different types of chemical bonding, such as ionic bonds, covalent bonds, hydrogen bonds, coordinate covalent bonds, etc., hold molecules to one another. While the infrared regime is where the frequency of these bonds' vibrational movements occurs. The infrared response of the sample is typically measured with a Michalson interferometer.

An infrared radiation source, an interferometer, and a detector make up an FTIR spectrometer. Infrared radiation is produced by an infrared radiation source and is transmitted by an interferometer. The interferometer then divides the infrared radiation beams, produces an optical path difference between the two beams, and because of the optical path difference from the detector, produces the interference signal. The detector

logs the sample's infrared response to a range of frequencies (wavenumbers) between 400 and 4000 cm^{-1} [8].

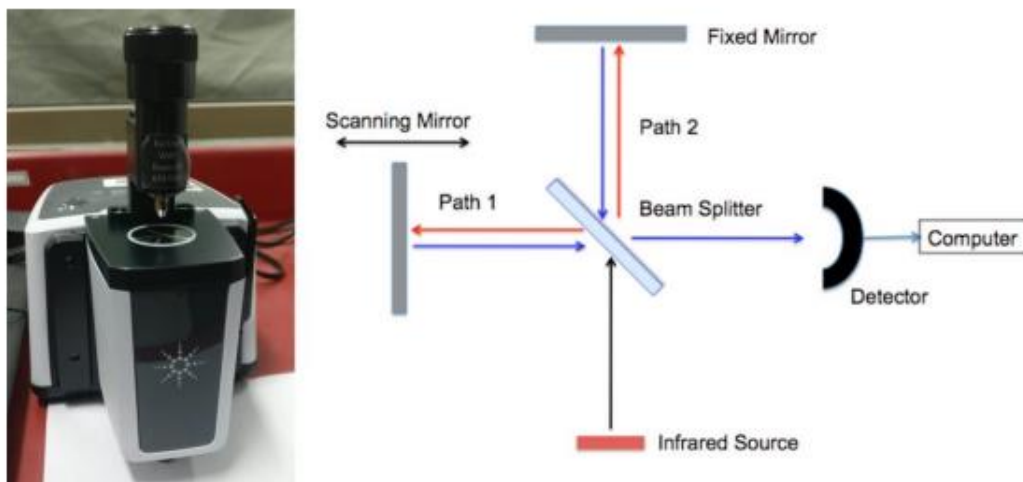


Figure 3.6. Schematic diagram of FTIR [9]

3.2.5. Water Contact Angle (WCA)

A technique for assessing a thin film's hydrophobic/hydrophilic behavior is contact angle measurement. By examining the behavior of solutions on the surface when they encounter the solid layer, it can also provide estimations for the roughness of a film. This device measures the angle at which the solid and liquid phases come into contact. A film that has been deposited has a hydrophobic behavior if the contact angle is larger than 90 [10].

A water drop with a predetermined size in microliters is dropped on the surface of the substrate while the sample is mounted on a mobile stage. The applied droplet and the sample are both illuminated by a light source. A predetermined time-stamped video is captured by a 60 fps camera positioned on the opposing side [11]. A manual dial on the apparatus, as depicted in Figure 3.8, can also be used to manually adjust the brightness of the image. The droplet's borders are then traced using built-in software tools, and the contact angle is then calculated automatically.

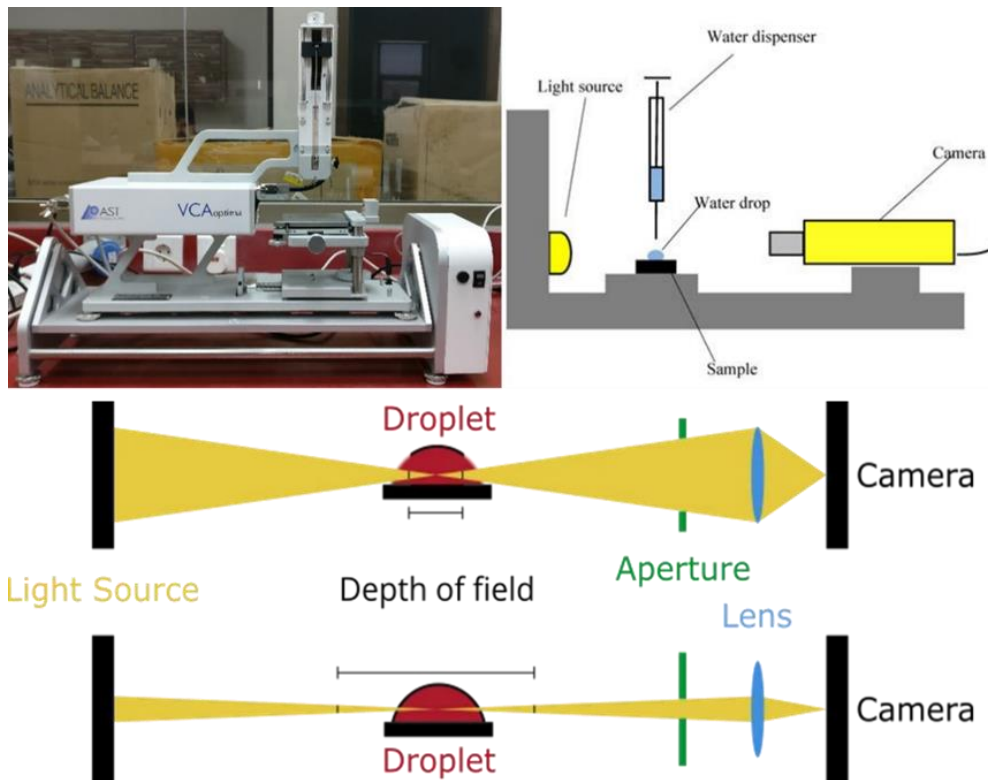


Figure 3.7. Schematic diagram and setup of water contact angle measurement[11]

3.3. Anti-Soiling Testing

3.3.1. Indoor Soiling Chamber

To research how soiling affects PV modules, the soiling chamber offers a controlled environment. It has an aluminum rod assembly for the door. An LTE floodlight and a glass cover provide additional lighting options in the chamber. It contains openings for a drawer, wire passage, soil pouring bin, and humidifier hose. The control unit includes a Peltier fan-connected temperature controller, ink bird humidity controller, and AC power supply. To produce soil clouds, an oil-free air compressor with a filter and regulator is utilized. A distribution box, a stand that can be adjusted, and dust vials for dirt containment are all included in the arrangement. The Ink Bird Humidity Controller regulates the humidity using a reptile fogger. Based on preset points, the temperature controller operates heating or cooling elements. A controlled and automated approach is offered by this soiling chamber to research the effects of soiling on PV modules[12].



Figure 3.8. Setup of Indoor Soiling Chamber[13]

3.3.2. IV-Curve Measurement using Solar Simulator

A light source called a solar simulator simulates the sunlight's radiance. Under regulated, repeatable laboratory circumstances, solar simulators with varying designed spectrum output are used to test several samples, including but not limited to solar cells, sunblock (SPF), materials photo-stability, and other samples (in-vivo or in-vitro)[14].

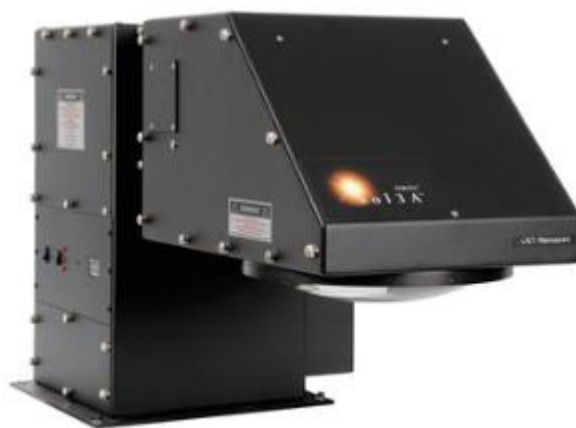


Figure 3.9. Oriel Sol3A simulator[14]

Solar simulators are tools that simulate sunlight's irradiance to evaluate photovoltaic (PV) modules. To achieve proper irradiance, the light source must be positioned with

respect to the sample stage when a solar simulator is set up. In contrast to collimated light beams, which travel in parallel rays to minimize spread, point light sources emit light uniformly in all directions. To correctly duplicate solar irradiance, LED arrays need separate power sources for each LED. Control elements and power supply differ depending on the light source. To enhance the reproduction of the sun spectrum and provide even lighting over the test area, optics, such as lenses and filters, are used[15].

Summary

In Chapter 3, deposition, characterization, and anti-soiling testing are discussed in relation to examining thin film optoelectronic capabilities. The electrospinning technique, which employs a high voltage power source to create nanofibers with a high surface area-to-volume ratio, is introduced in the first section of the chapter. The method of using plasma cleaning to clean substrate surfaces and improve adhesion prior to thin film deposition is then covered. The chapter also discusses characterization methods including UV-VIS-NIR spectroscopy, which studies a material's response to light spectrum, and X-ray diffraction (XRD), which investigates the structural and crystallographic properties of samples. The morphology of a specimen is imaged and studied using scanning electron microscopy (SEM), while chemical interactions are examined using Fourier transform infrared spectroscopy (FTIR). The chapter ends with a discussion of an indoor soiling chamber, an IV-curve measurement utilizing a sun simulator for anti-soiling testing, and a contact angle measurement to evaluate film hydrophilicity. The processes and methodologies utilized in the deposition, characterization, and testing of thin films for optoelectronic applications are covered in detail in this chapter.

References

- [1] M. Q. Khan *et al.*, “Self-cleaning properties of electrospun PVA/TiO₂ and PVA/ZnO nanofibers composites,” *Nanomaterials*, vol. 8, no. 9, Sep. 2018, doi: 10.3390/nano8090644.
- [2] Y. Z. Long, X. Yan, X. X. Wang, J. Zhang, and M. Yu, “Electrospinning,” in *Electrospinning: Nanofabrication and Applications*, Elsevier, 2018, pp. 21–52. doi: 10.1016/B978-0-323-51270-1.00002-9.
- [3] “X-ray diffraction _ Definition, Diagram, Equation, & Facts _ Britannica”.
- [4] “X-ray Powder Diffraction (XRD)”.
- [5] “Lambert Law - an overview _ ScienceDirect Topics”.
- [6] “UV-3600i Plus - Features _ Shimadzu Scientific Instruments”.
- [7] “Scanning Electron Microscopy - Nanoscience Instruments”.
- [8] A. Dutta, “Fourier Transform Infrared Spectroscopy,” in *Spectroscopic Methods for Nanomaterials Characterization*, Elsevier, 2017, pp. 73–93. doi: 10.1016/B978-0-323-46140-5.00004-2.
- [9] “14. Fourier Transform Infrared Spectroscopy (FTIR) - Chemistry LibreTexts”.
- [10] “Contact Angle Measurement, Theory & Relation to Surface Energy _ Ossila”.
- [11] “Contact angle of copper-bearing shales using the sessile drop and captive bubble methods in the presence of selected frothers _ Semantic Scholar”.
- [12] N. Hussain and N. Shahzad, “Design of Homemade Soiling Station to Explore Soiling loss effects on PV Module,” 2021.
- [13] N. Hussain *et al.*, “Designing of homemade soiling station to explore soiling loss effects on PV modules,” *Solar Energy*, vol. 225, pp. 624–633, Sep. 2021, doi: 10.1016/j.solener.2021.07.036.
- [14] “Solar Simulator Selection Guide”.
- [15] “Solar Simulator Design, Working Principles & Optics _ Ossila”.

Chapter: 4 Experimental Work

This chapter illustrates the experimental work performed to prepare electrospun TiO₂/SiO₂ thin films on glass substrate and performed characterization techniques to study different properties and finally to analyze the self-cleaning behavior, the films were soiled in homemade soiling chamber.

4.1. Materials

Titanium (IV) Isopropoxide (TTIP, $\geq 95\%$ pure) from Alfa Aesar and Tetraethyl Orthosilicate (TEOS, $\geq 97\%$ pure), Polyvinylpyrrolidone (PVP) ($M_w = 90,000$), Ethanol (purity= 99.9%), and Acetic Acid (purity=100%) from Sigma Aldrich were purchased and were used as it is without any further purification.

4.2. Preparation of the precursor solution for Electrospinning

A solution containing tetraethyl orthosilicate (TEOS) and titanium isopropoxide (TTIP) was prepared as a composite solution, with three different volume ratios: TiO₂-SiO₂ (3:1), TiO₂-SiO₂ (1:1), and TiO₂-SiO₂ (1:3). Additionally, a pristine TiO₂ solution was prepared for comparison purposes.

To prepare the TiO₂:SiO₂ (1:1) solution, 0.5 mL of TTIP and 0.5 mL of TEOS were added to 9 mL of ethanol, followed by 3 mL of acetic acid. The resulting solution was stirred at room temperature until the TTIP was fully hydrolyzed. Next, 0.55 g of polyvinylpyrrolidone (PVP) was added gradually to the solution while stirring, and the stirring continued until a homogenous solution was achieved shown in figure 4.1. The other two ratios were prepared similarly, with the only difference being the amount of TEOS added in the first step.

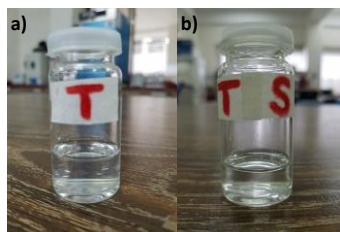


Figure 4.1. Electrospinning solution of a) TiO_2 b) TiO_2 - SiO_2 composite

4.3. Substrate Preparation

The soda lime glass and Low iron float glass (7cm x 2.5cm) were subjected to a thorough cleaning process prior to electrospinning. This involved immersing them in de-ionized water, acetone, ethanol, and iso-propanol for approximately 10 minutes each using ultrasonic equipment. To further ensure that the glass surfaces were free from any impurities, they were treated in a plasma cleaner for 10 minutes. After that glass plates were promptly utilized for coating via electrospinning.

4.4. Fabrication of TiO_2 - SiO_2 Nanofibers

The synthesis process of the fabrication of TiO_2 - SiO_2 composite nanofibrous films is illustrated in the schematic diagram below in figure 1. Electrospinning was done using FLUIDNATEK (LE-10) from Bioinicia. 5ml plastic syringe was filled with the above prepared solution and the syringe is then installed on the syringe pump. The distance between the nozzle and the collector plate was kept at around 15cm, flow rate was 1ml/hr and the voltage was set at 10KV for electrospinning. For optimization, electrospinning was done for 3 and 5 minutes. Subsequently, composite nanofibers were collected on the glass slides mounted on the flat plate collector. After that, the coated glass slides were calcinated at 180 °C for 2 hrs followed by annealing at 500 °C for 2 hrs for complete evaporation of PVP to obtain TiO_2 - SiO_2 nanofibrous thin films on glass substrate.

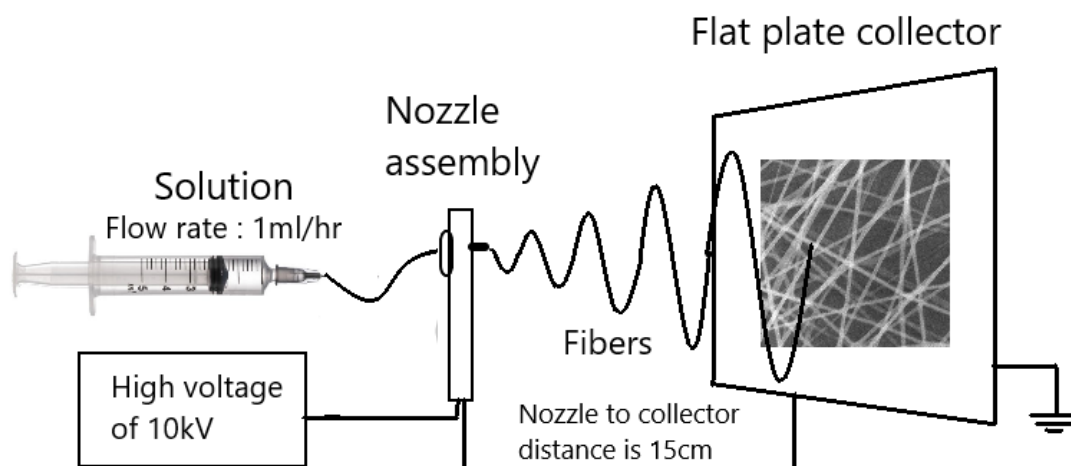


Figure 4.2. Schematic showing nanofiber fabrication through electrospinning

4.5. Film Characterizations

A range of characterization methods have been utilized to examine the film's structure and morphology, its composition, as well as its hydrophobic and hydrophilic traits, in addition to its self-cleaning property by testing in soiling chamber.

Utilizing X-ray Diffraction (XRD) analysis on a Bruker D8 Advanced equipment, with a scan rate of $1.25^\circ/\text{min}$ and a 2θ range from 10° to 80° , the structural properties and crystallite sizes of the films were examined. Cu K radiation ($\lambda = 1.542$) was used with an activation voltage of 40 kV and a current of 30 mA. Signal processing and peak estimation were done using MDI's Jade 6.5 program.

The morphology of the thin films on glass surface were examined using scanning electron microscope (SEM) MIRA3 TESCAN operating at 10 kV. Using a UV-3600 Plus Ultraviolet-Visible NIR Spectrophotometer with a 2.5 m slit width, the optical characteristics of thin films were examined. In the 250-1100 nm wavelength range, transmittance and absorbance measurements were made.

Fourier-transform infrared spectroscopy (FTIR) investigations were carried out utilizing the CARY 630 FTIR from Agilent Technologies, USA, to examine intermolecular interactions. The wavenumber range was maintained between 4000 and 640 cm^{-1} , and the diamond ATR module was used.

Using a $30\ \mu\text{L}$ droplet of de-ionized water, a VCA Optima device from ASTP was employed for contact angle analysis under typical atmospheric circumstances.

4.6. Anti-Soiling Testing

4.6.1. Soiling

The prepared coatings on glass slides were tested for self-cleaning in an indoor self-made soiling station(Hussain et al. 2021, 2022). The effect of the coatings on soiling was tested for three different tilt angles (0° , 33.4° and 60°). The coated and uncoated glass slides were placed on an adjustable aluminum stand within the chamber. The humidity level within the chamber was raised to 70% using a Reptile fogger. 2g of soil, collected from the solar panels, was measured, and kept in the dust vial. To disperse the soil, compressor's push button valve was pressed for 2s while the air pressure being kept at 30 psi. The glass slides were given 10 mins to allow the soil particles to completely deposit. Now the temperature within the chamber using Thermoelectric Peltier elements was raised to 50°C and was maintained for a total of 10 mins followed by cooling the glass slides at room temperature. After that the weight of the soiled samples were measured. This cycle was repeated 4 times to acquire four layers of soil on the glass slides.

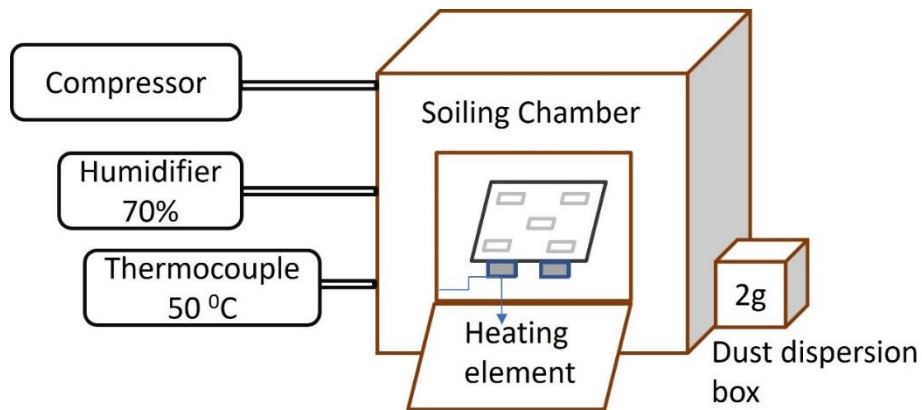
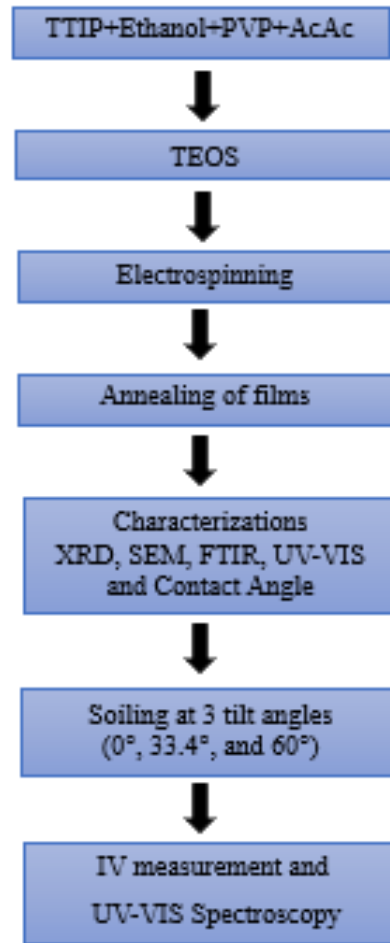


Figure 4.3. Schematic showing the setup of indoor soiling chamber

4.6.2. IV-Curve Measurement

Class AAA solar simulator from oriel instruments is used to measure the IV characteristics by placing the glass slides coated with the anti-soiling coating on a mini PV module.

Flow chart



Summary

The experimental work done to create TiO₂/SiO₂ thin films on glass substrates using electrospinning is described in Chapter 4. Tetraethyl orthosilicate (TEOS) and titanium isopropoxide (TTIP) were mixed in various volume ratios to create the precursor solution. The solution was electrospun onto glass slides, which were then dried and annealed to create the films. The films were analyzed using a variety of characterization methods, including X-ray diffraction (XRD) for structural properties, scanning electron microscopy (SEM) for morphology, ultraviolet, visible, and near-infrared (UV-VIS-NIR) spectroscopy for optical properties, Fourier transform infrared spectroscopy (FTIR) for intermolecular interactions, and contact angle measurement for hydrophobicity/hydrophilicity. Additionally, the films' capacity for self-cleaning was examined by soiling them in a constructed chamber, followed by weight and Isc

measurements. The use of a Class AAA solar simulator to gauge the IV properties of coated glass slides mounted on a tiny PV module is mentioned as the chapter ends.

Chapter: 5 Results and Discussion

The study's findings are clarified in the results and discussion chapter, along with their significance in relation to the study's goals. The many surface, structural, chemical, and optical characteristics of the pure and composite thin films are comprehensively examined and addressed through the evaluation of data obtained from a variety of characterization techniques.

5.1. Structural Analysis

The crystal structures of the prepared samples with varied TiO_2 - SiO_2 compositions were analyzed by using X-ray diffraction. Fig. 5.1. displays the XRD spectrum of pristine TiO_2 and TiO_2 - SiO_2 composite nanostructured films. The XRD peaks centered at $2\theta = 25.28^\circ$, 37.8° , 48.04° , 55.06° and 62.68° correspond to hkl values of (101), (112), (200), (211) and (204) tetragonal crystal planes of anatase TiO_2 which is highly beneficial for self-cleaning and photocatalytic property. The diffraction peaks seen in the sample of pure TiO_2 are consistent with those on JCPDS Card No. 21-1272.

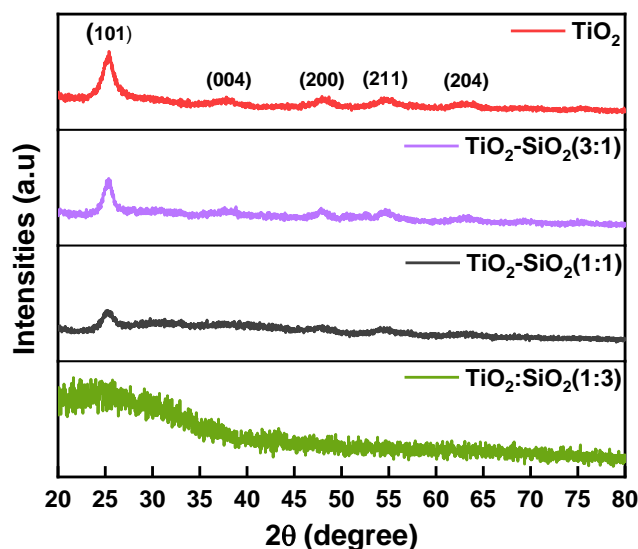


Figure 5.1. XRD plots of the annealed thin films at 500 °C

However, when SiO_2 is added to TiO_2 , only the (101) peak retains its prominence, and the peaks corresponding to the anatase phase of titania grow wider and less pronounced. Other peaks that were visible in the sample of pure TiO_2 progressively vanish as well. This can be explained by the fact that SiO_2 inhibits the growth of

anatase TiO₂ when its ratio increases. Moreover, TiO₂-SiO₂ nanostructured composites do not exhibit any SiO₂ diffraction peaks, which may be due to the amorphous nature of silica[1].

5.2. Transmittance Results

Fig. 5.2. shows the UV-VIS transmittance spectra and Tauc plots of the developed anti-soiling coatings. In the UV-Vis band in Fig 5.2.a and 5.2.c, all the nanocomposite's coatings displayed transmittance ranging from 80 to 90% in the visible region (400nm-700nm) when electrospinning was done for 3min and 76 to 87% for 5mins. Figure 5.2.a, and c demonstrates that transmittance increases with increasing the SiO₂ content with values calculated as 83.1%, 86.8%, 86.9%, and 89.5% and 76.9%, 85.5%, 85.7% and 86.4% when electrospinning was done for 3 and 5 minutes respectively. The former case was more comparable to the transmittance of uncoated substrate i.e., 88.9%. These findings are consistent with the information provided by Chatterjee et al. [2] and Zhang et al. [3] which demonstrates that compared to pristine TiO₂, the composite show higher transmittance. In the case of solar photovoltaic panels, the optical transmittance of the self-cleaning or anti-soiling coating is of utmost importance so it is desirable to have optical transmittance same or greater than the solar glass itself that is why the former case is selected for further investigation.

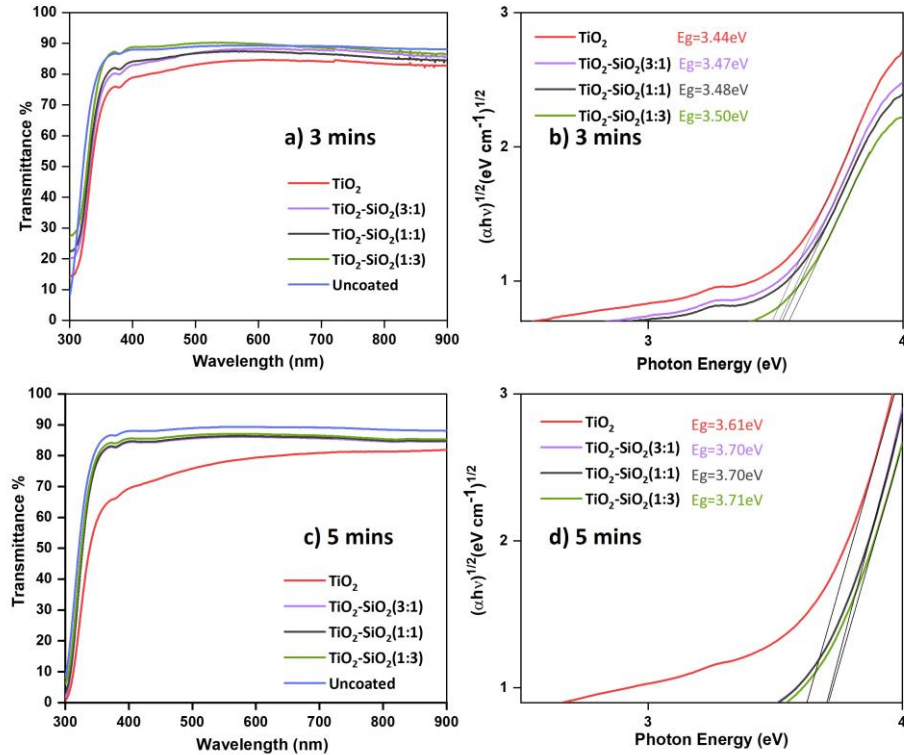


Figure 5.2. Optical transmittance and Tauc plot curves obtained after 3 mins (a, b) and 5 mins (c, d) of electrospinning

Based on our results, the coating with the highest silica content achieved optical transmission greater than the uncoated glass i.e., 88.9%. Due to the higher refractive index of 2.52, TiO₂ thin film has 5.8% less transmittance in the spectrum than the glass. In comparison, the composites show increased transmittance because SiO₂ has a lower refractive index than TiO₂[3]. For optical bandgap assessment, Tauc plots in Figure 5.4 b, and d. between the absorption coefficient $(\alpha h\nu)^n$ (where $n=1/2$ for indirect optical transition) and photon energy ($h\nu$) were used which resulted in values of 3.44 eV, 3.47 eV, 3.48 eV, and 3.50 eV for TiO₂, TiO₂-SiO₂ (3:1), TiO₂-SiO₂ (1:1), and TiO₂-SiO₂ (1:3), respectively. The band gap energy has increased from 3.44 to 3.50 eV. The higher band gap for the composite with ratio (1:3) can be attributed to the amorphous nature of the composite as depicted in XRD analysis. The band gap range observed for amorphous TiO₂ is from 3.30 to 3.5eV. The rest of the coatings show band energies corresponding to the crystalline anatase structure of TiO₂, which is highly favored for self-cleaning applications[4].

5.3. Chemical Analysis

The FTIR spectra of temperature annealed and non-annealed composite nanofibers was studied in fig. 5.3. for chemical structure analysis. The non-annealed nanofibers show the characteristic peaks at 1277, 1436, 1652, 2900 and 3360 cm^{-1} . The peak at 1652 cm^{-1} is an indication of stretching vibration of C=O carbonyl group in PVP whereas peak at 1277 cm^{-1} indicates the mode of C-N bond stretching[5][6]. The band centered around 1634 cm^{-1} in annealed nanofibers presumably corresponds to the bending vibrations of O-H. The composite film, on the other hand, reveals no peak (annealed at 500 °C), proving that all the organic components from PVP have evaporated during the annealing process. The broad absorption at 3000-3400 cm^{-1} can be assigned to the stretching vibrations of O-H bonds, resulting from adsorbed moisture at the surface. The stretching vibration of the -CH₃ was linked to the broad peak at 2900 cm^{-1} [7] .

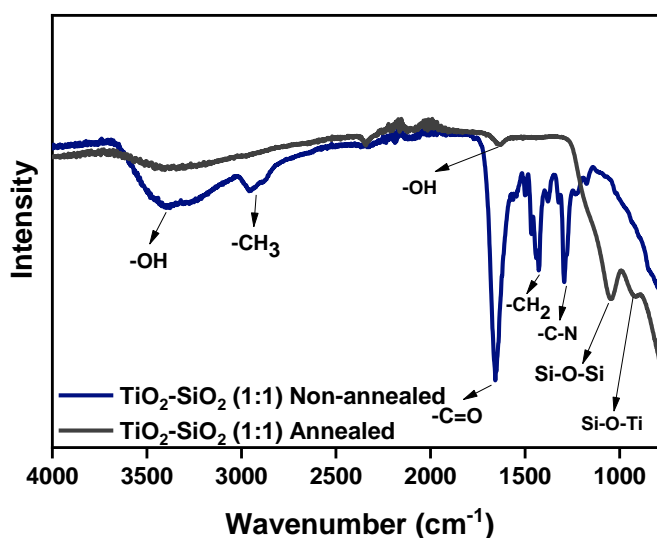


Figure 5.3. FTIR spectra of temperature non-annealed and annealed $\text{TiO}_2\text{-SiO}_2$ (1:1) nanofibrous thin film

In addition, the peak at 1400 cm^{-1} is the vibration of the CH₂ bond from PVP[5]. The band at 1041 cm^{-1} and around 930 cm^{-1} can be attributed to the asymmetrical stretching vibrations of the Si–O–Si framework and Si-O-Ti respectively[8][9][10]. The presence and stretching of hydroxyl groups in the FTIR study serve to confirm the hydrophilic behavior of the films.

5.4. Wettability Study

Fig. 5.4. shows the water contact angle for pristine TiO_2 films and TiO_2 - SiO_2 nanostructured composite films at an annealing temperature of 500 °C. For the pristine TiO_2 and TiO_2 - SiO_2 composite films for the ratios (3:1), (1:1), (1:3), the water contact angle was measured to be 29.1°, 14.5°, 11.3°, and 18.7° respectively.

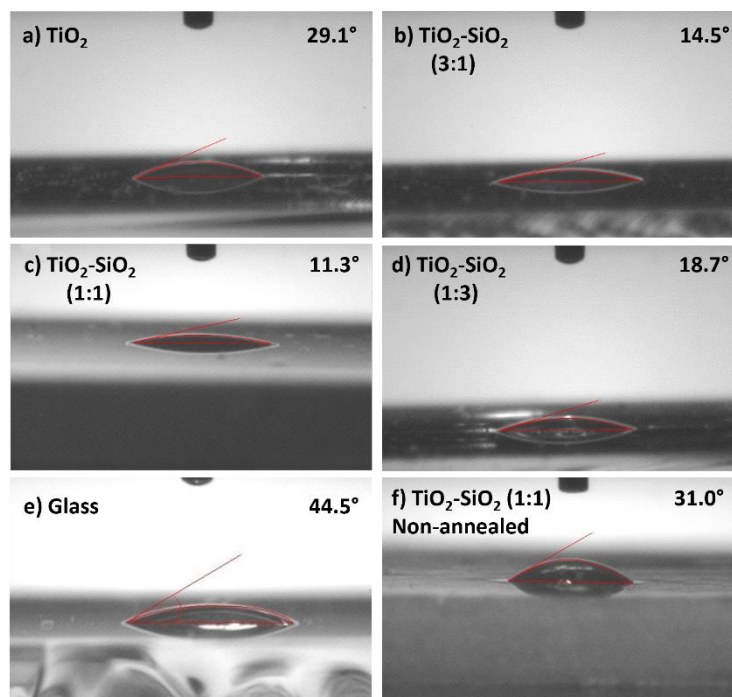


Figure 5.4. Water contact angle measurements of TiO_2 and TiO_2 - SiO_2 thin films

The results indicate that the nanostructured composite film was hydrophilic. This hydrophilic nature can be the result of greater amount of hydroxyl groups due to bronsted acidity induced by SiO_2 component in the film[11]. These hydroxyl groups help in slowing down the electron-hole pair recombination by trapping the photogenerated electrons. The charge on electron and holes helps in adsorption of water molecules at the defect sites and enhance the hydrophilic nature even in the darker environment[12]. According to the results, TiO_2 - SiO_2 composite film with a volume ratio of (1:1) annealed at 500° C is the most hydrophilic when compared to other samples.

5.5. Morphological Analysis

Fig. 5.6. displays the scanning electron microscopy (SEM) images of pristine TiO_2 and TiO_2 - SiO_2 composite nanofibrous films coated on PV glass cover. The images reveal

that the annealing of nanofibers resulted in randomly orientated and well-connected networks.

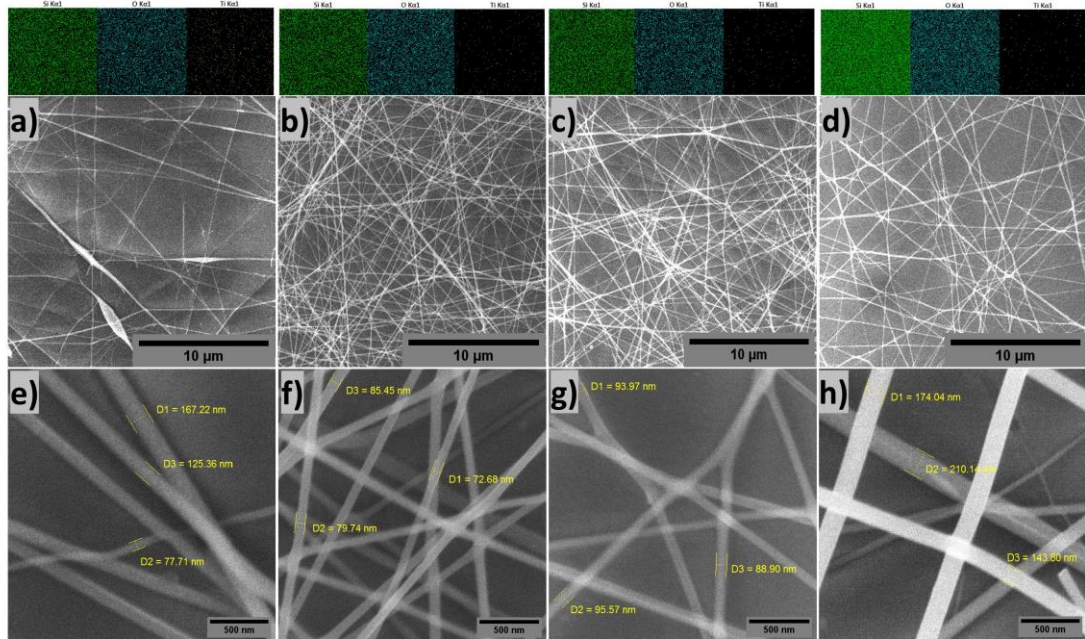


Figure 5.5. SEM images of a) TiO_2 , c) $\text{TiO}_2\text{-SiO}_2(3:1)$, e) $\text{TiO}_2\text{-SiO}_2(1:1)$, g) $\text{TiO}_2\text{-SiO}_2(1:3)$ nanofibrous thin films and their respective close view b, d, f and h) and Elemental mapping results above

The diameter ranges from 70-170nm, 70-85nm, 88-95nm and 140-210nm for TiO_2 , $\text{TiO}_2\text{-SiO}_2(3:1)$, $\text{TiO}_2\text{-SiO}_2(1:1)$, and $\text{TiO}_2\text{-SiO}_2(1:3)$ respectively. Overall, there is an increase in the fiber diameter hence decrease in the density of the nanostructure network. This increase is due to the changing viscosity of the solution with silica addition. Higher viscosity leads to fibers with larger diameters as the charge may not be enough to stretch the polymer solution to the appropriate fiber diameter[13]. In the case of pristine TiO_2 , the fibers diameter becomes less uniform, and beads have also appeared maybe because there was not enough sol-gel viscoelastic force to counteract the repelling forces of charge resulting in localized thickening in some regions[14]. It is evident from fig. 5.5. (e, f, g. and h) that combining silica with titania has resulted in uniform nanofiber formation and improved film density which enhances the hydrophilicity (as evidenced by a decrease of WCA promoting faster water chemisorption leading to improved self-cleaning properties[15]). However, with a very high silica content the fiber diameter has increased, becomes non-uniform and film becomes less dense. These results are in line with what Shahhosseininia et al. has to said[16]. The elemental distribution of the pristine TiO_2 and $\text{TiO}_2\text{-SiO}_2$ nanofibers is

also shown in fig. 5.5 above the respective samples. The mapping analysis shows a homogenous distribution of elements and change can be observed with the varying ratio of the elements. Si and O content seems too high because of the glass substrate.

5.6. Soiling Study in Indoor Conditions

The effectiveness of the developed coatings was investigated in indoor soiling stations which is quick process, and the conditions can be properly monitored.

5.6.1. Analysis of soiling density under different tilt angles

Since the tilt angle can reduce the dust deposition due to gravitation, the effect of tilt angle was studied on spectral transmittance degradation, soiling density, and power loss of the hydrophilic coatings.

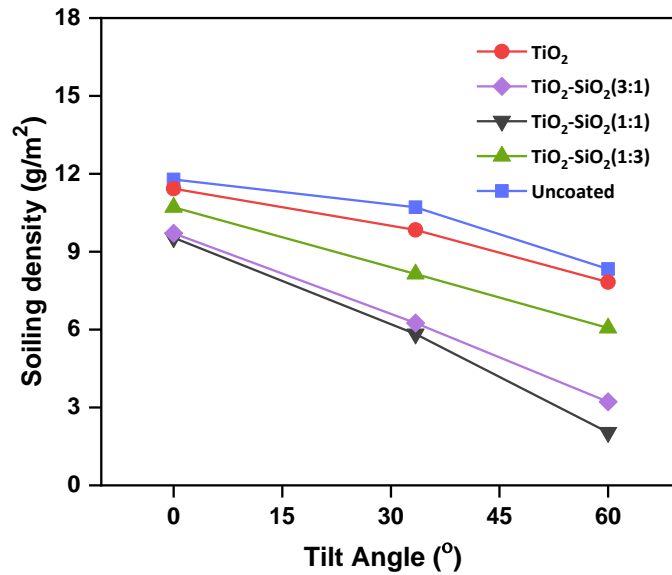


Figure 5.6. Soil deposition density vs Tilt angle

Fig. 5.6. shows the soiling density on the PV cover glass under tilt angles of 0°, 33.4°, and 60° obtained after 4 daily soil cycles as per equation 1.

$$\text{Soiling Density}(g/m^2) = \frac{W_a - W_b}{A} \quad (1)$$

W_a is the weight of the glass substrate after soiling

W_b is the weight of the glass substrate before soiling

A is the area of glass substrate

It is obvious that soil density is higher for smaller tilt angle. When the tilt angle is 0° , the soiling density for uncoated, TiO_2 and $\text{TiO}_2\text{-SiO}_2$ (1:3) glass is more than the other samples because they were placed closer to the dust dispersion box. As can be seen from fig.5.6, the soiling density on the uncoated glass substrate is more than the glass with the hydrophilic coatings thereby supporting the quantitative findings of lower transmittance found in fig. 5.7. From the tilt angle of 0° to 33.4° , the reduction in soiling density ranges from 9% to 39% and from the tilt angle of 33.4° to 60° , it ranges from 20% to 65% for all nanocoatings. The change in soiling density reduction for higher tilt angle is more, due to the combined effects of gravity and soil-surface adhesion, these soil particles that detach onto sloped surfaces may roll or slide down the surface[17]. It can be due to the presence of nanofibers on the hydrophilic surface. The nanofibers induce a certain level of surface roughness due to their randomly orientated network which decreases the adhesive forces between the soil particles and coated surface[18]. For the ratio (1:3), the soiling density was more which can be attributed to the amorphous nature of the sample as well as the increase in fiber diameter which increases the contact area for soil particles to adhere to the surface of thick fiber. Overall, the results indicates that dust deposition can be reduced by hydrophilic coatings to a certain degree even without water showering[19].

5.6.2. Analysis of direct transmittance after soiling

The direct transmittance results obtained after 4 daily soil cycles (2g/each) onto the PV cover glass were analyzed in fig. 5.7. For tilt angles 60° , 33.4° , and 0° , $\text{TiO}_2\text{-SiO}_2$ (1:1) exhibit 16.1%, 16.5%, and 7% greater transmittance in the visible region (400-700nm) than the uncoated glass after soiling respectively. The results also indicate that with increasing the tilt angle, the transmittance increases as the soiling density decreases.

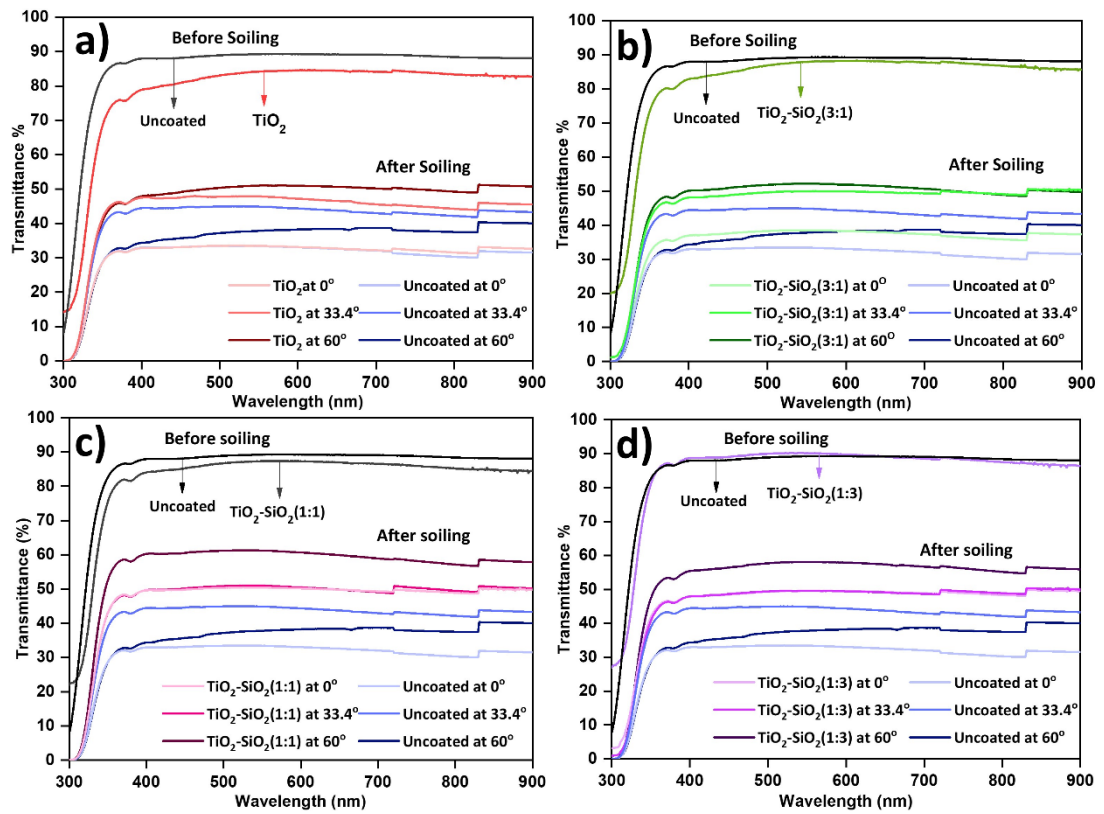


Figure 5.7. Optical transmittance results of a) TiO_2 , b) $\text{TiO}_2\text{-SiO}_2$ (3:1), c) $\text{TiO}_2\text{-SiO}_2$ (1:1) d) $\text{TiO}_2\text{-SiO}_2$ (1:3) obtained after soiling under tilt angles of 0° , 33.4° and 60°

According to the results, the highest drop in transmittance is for $\text{TiO}_2\text{-SiO}_2(3:1)$ and pristine TiO_2 due to more soil deposited on the substrate as evidenced from fig. 5.6. Overall, the results indicate a clear relation between optical transmittance and soiling density. Although there is a significant drop in transmittance after soiling, all samples show higher optical transmittance than that for the uncoated glass.

5.6.3 I-V characteristics and Current Density Analysis

In order to assess the feasibility of incorporating an optically transparent, hydrophilic coated glass substrates as PV glass cover, the coated substrates were placed on top of a commercially available mini solar cell and its photovoltaic properties were measured. Fig. 5.8. represents the current-voltage (I-V) curves of uncoated and hydrophilic coatings after soiling. The cell efficiency of the solar cell covered with uncoated glass substrate was 5.3%.

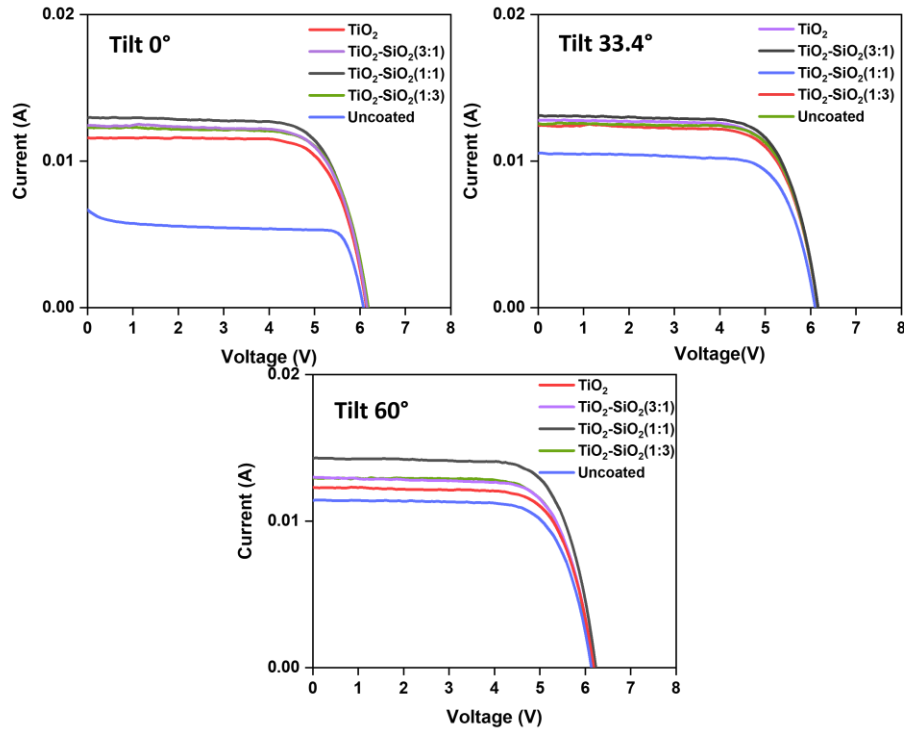


Figure 5.8. I-V curves for the $\text{TiO}_2\text{-SiO}_2$ films under tilt angles of 0° , 33.4° and 60°

Generally, all coatings showed better solar efficiency compared to the uncoated substrate after soiling but the maximum increase in efficiency is obtained at 60° tilt because at higher tilt both the influence of gravity and anti-soiling coating helps in rolling or sliding of soil, facilitating the self-cleaning effect. From the figure 5.8, it can be seen that the current was the most affected by soil deposition because under mild shadowing conditions brought on by soiling, output current varies significantly but the output voltage will remain relatively constant[20]. On uncoated glass substrate, it was evident that the decline in PV efficiency grew as the tilt angles were lowered. The reason for this was that when the tilt angle decreased, more dust was deposited on glass. At 0° tilt, the change observed is only due to the placement of the samples in the chamber since samples placed close to the dust dispersion box experienced greater soil exposure thus lowered efficiency. When the tilt angle was 33.4° , the PV efficiency for uncoated substrate was 3.3% and on coated surfaces (3.9%-4.2%). When the tilt angle was increased to 60° , the PV efficiency for uncoated glass substrate was 3.6% and (3.9%-4.6%) for coated surface. For both 33.4° and 60° , the optimal performance was exhibited by $\text{TiO}_2\text{-SiO}_2$ (1:1) substrate which showed an increase in efficiency to 4.2%, and 4.6% in comparison to uncoated substrate having efficiency of 3.3% and 3.6%

respectively. $\text{TiO-SiO}_2(1:1)$ showed 29.8% (33.4°) and 42.7% (60°) less soiling density than the glass substrate.

The PV efficiency reduction for the glass substrate for the tilt 33.4° is 2% and 1.7% for the tilt 60° . In contrast, the coating having $\text{TiO}_2\text{-SiO}_2$ ratio (1:1) shows PV efficiency reduction of 1.1% and 0.7% respectively. The current density (J_{sc}) is also represented in the bar graph for each sample in fig. 5.9. For samples with higher soiling density, the current density (J_{sc}) is decreasing due to decreased light absorption.

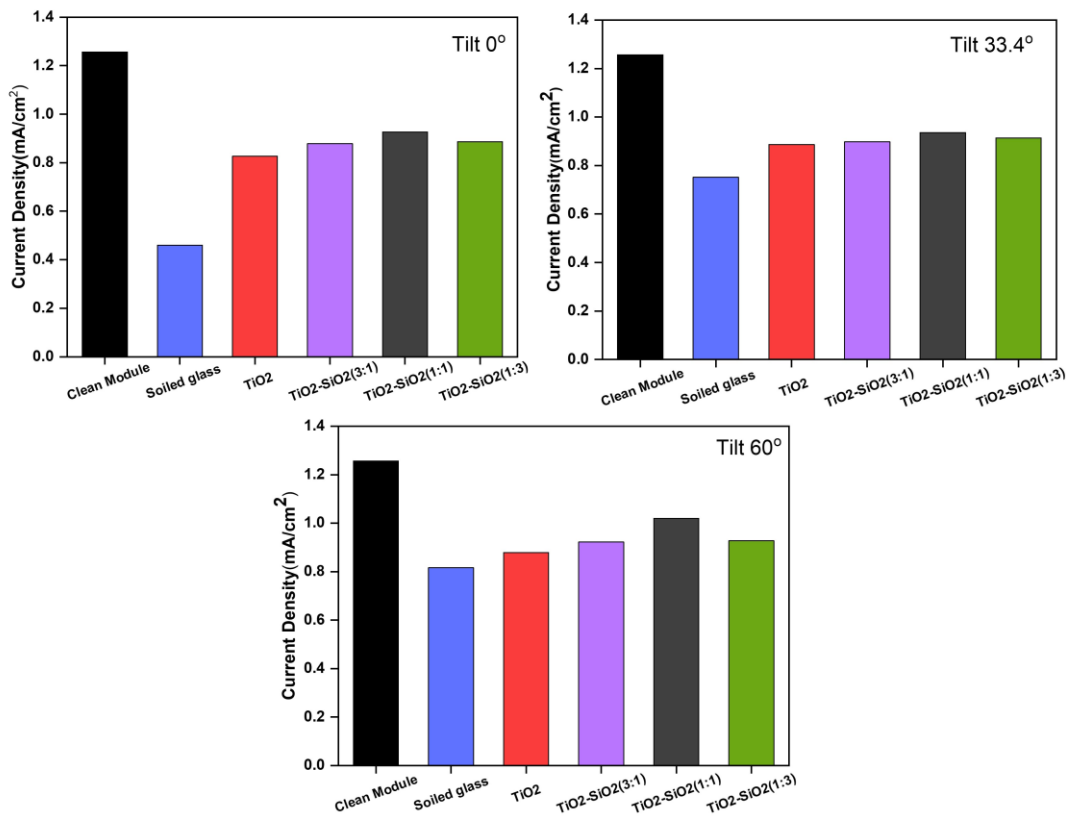


Figure 5.9. Current density analysis of the developed coatings for all three tilt angles

The highest J_{sc} is seen for the $\text{TiO}_2\text{-SiO}_2$ formulated ration of (1:1) i.e., $1.019 \text{ mA}/\text{cm}^2$ greater than the uncoated glass which has J_{sc} of $0.8159 \text{ mA}/\text{cm}^2$. J_{sc} is directly dependent on the transmittance of the samples which in turn depends on the soiling density. Overall, the J_{sc} is higher for the coated samples in comparison to the uncoated glass.

5.7. Comparison of this study with the reference studies

Table 1. 1. The summary of the water contact angle and transmittance enhancement of the coatings before and after soiling.

<i>S#</i>	<i>Deposition method</i>	<i>Transmittance after deposition%</i>	<i>Transmittance enhancement after soiling/%</i>	<i>WCA/°</i>	<i>Reference</i>
1	Dip coating	-	>8	29.0	[21]
2	Spin coating	70.0	-	37.3	[22]
3	E-beam	86.3	>8	-	[23]
4	Spray coating	88.7	-	22.7	[24]
5	Dip coating	84.0	>6	44.0	[25]
6	Electrospinning	86.9	>16	11.3	This study

In short, the fabrication of TiO₂-SiO₂ nanofibrous coating by electrospinning has a lot of potential to be a solar panel cover glass coating with transparent, self-cleaning hydrophilic properties.

Summary

The study's conclusions about pure and composite thin films were presented and discussed in Chapter 5, which is devoted to results. An X-ray diffraction structural examination of the composites showed that the addition of SiO₂ to TiO₂ prevented the formation of anatase TiO₂, which gave rise to their amorphous character. The TiO₂-SiO₂ composite films had better transmittance than uncoated glass, according to the results of the study, with the greatest transmittance being attained at a certain SiO₂ percentage. The elimination of organic components during annealing and the existence of hydroxyl groups, which indicate hydrophilicity, were both verified by chemical analysis using FTIR spectroscopy. The hydrophilic character of the composite films was shown by a wettability analysis, which was explained by the presence of hydroxyl groups produced by SiO₂. With the addition of SiO₂, morphological examination

revealed well-connected networks of nanofibers with increased diameter and decreased density. According to a soiling investigation, the composite films showed less soiling density than uncoated glass, and the difference became more pronounced at greater tilt angles. The composite films retained greater transmittance than the uncoated glass, according to an analysis of direct transmittance after soiling. After soiling, I-V characteristics showed that coated substrates had higher solar efficiencies than untreated glass, with the $\text{TiO}_2\text{-SiO}_2$ (1:1) composite showing the greatest improvement. Overall, the results show that $\text{TiO}_2\text{-SiO}_2$ nanocomposite coatings have good qualities and may be used to create hydrophilic coverings that are self-cleaning for photovoltaic glass applications.

References

- [1] M. Zhang, L. E. R. Zhang, and Z. Liu, "The effect of SiO₂ on TiO₂-SiO₂ composite film for self-cleaning application," *Surfaces and Interfaces*, vol. 16, pp. 194–198, Sep. 2019, doi: 10.1016/j.surfin.2018.10.005.
- [2] K. Chatterjee, S. Ray, B. Pal, K. Adhikary, U. Gangopadhyay, and R. Mandal, "A comparative study of SiO₂:TiO₂ composite and SiO₂ film by sol-gel method for solar cell application," in *Springer Proceedings in Physics*, Springer Science and Business Media, LLC, 2019, pp. 341–347. doi: 10.1007/978-3-319-97604-4_52.
- [3] M. Zhang, L. E. R. Zhang, and Z. Liu, "The effect of SiO₂ on TiO₂-SiO₂ composite film for self-cleaning application," *Surfaces and Interfaces*, vol. 16, pp. 194–198, Sep. 2019, doi: 10.1016/j.surfin.2018.10.005.
- [4] H. Albetran, B. H. O'Connor, and I. M. Low, "Effect of calcination on band gaps for electrospun titania nanofibers heated in air-argon mixtures," *Mater Des*, vol. 92, pp. 480–485, Feb. 2016, doi: 10.1016/j.matdes.2015.12.044.
- [5] M. Akhlaq and Z. S. Khan, "Synthesis and characterization of electro-spun TiO₂ and TiO₂-SnO₂ composite nano-fibers for application in advance generation solar cells," *Mater Res Express*, vol. 7, no. 1, 2020, doi: 10.1088/2053-1591/ab68a1.
- [6] T. Balkan, Z. Guler, M. Morozova, P. Dytrych, O. Solcova, and A. S. Sarac, "The effect of deposition on electrochemical impedance properties of TiO₂/FTO photoanodes," *J Electroceram*, vol. 36, no. 1–4, pp. 102–111, Jun. 2016, doi: 10.1007/s10832-016-0021-6.
- [7] Y. Yuan, Y. Duan, Z. Zuo, L. Yang, and R. Liao, "Novel, stable and durable superhydrophobic film on glass prepared by RF magnetron sputtering," *Mater Lett*, vol. 199, pp. 97–100, Jul. 2017, doi: 10.1016/j.matlet.2017.04.067.
- [8] M. J. Powell *et al.*, "Intelligent Multifunctional VO₂/SiO₂/TiO₂ Coatings for Self-Cleaning, Energy-Saving Window Panels," *Chemistry of Materials*, vol. 28, no. 5, pp. 1369–1376, Mar. 2016, doi: 10.1021/acs.chemmater.5b04419.
- [9] D. Adak *et al.*, "Self-cleaning V-TiO₂:SiO₂ thin-film coatings with enhanced transmission for solar glass cover and related applications," *Solar Energy*, vol. 155, pp. 410–418, 2017, doi: 10.1016/j.solener.2017.06.014.

- [10] F. Huang, B. Motealleh, W. Zheng, M. T. Janish, C. B. Carter, and C. J. Cornelius, “Electrospinning amorphous SiO₂-TiO₂ and TiO₂ nanofibers using sol-gel chemistry and its thermal conversion into anatase and rutile,” *Ceram Int*, vol. 44, no. 5, pp. 4577–4585, Apr. 2018, doi: 10.1016/j.ceramint.2017.10.134.
- [11] M. Zhang, L. E, R. Zhang, and Z. Liu, “The effect of SiO₂ on TiO₂-SiO₂ composite film for self-cleaning application,” *Surfaces and Interfaces*, vol. 16, pp. 194–198, Sep. 2019, doi: 10.1016/j.surfin.2018.10.005.
- [12] M. A. M. L. de Jesus, G. Timò, C. Agustín-Sáenz, I. Braceras, M. Cornelli, and A. de M. Ferreira, “Anti-soiling coatings for solar cell cover glass: Climate and surface properties influence,” *Solar Energy Materials and Solar Cells*, vol. 185, pp. 517–523, Oct. 2018, doi: 10.1016/j.solmat.2018.05.036.
- [13] Y. Z. Long, X. Yan, X. X. Wang, J. Zhang, and M. Yu, “Electrospinning,” in *Electrospinning: Nanofabrication and Applications*, Elsevier, 2018, pp. 21–52. doi: 10.1016/B978-0-323-51270-1.00002-9.
- [14] U. Abdillah *et al.*, “The effect of various electrospinning parameter and sol-gel concentration on morphology of silica and titania nanofibers,” *IOP Conf Ser Mater Sci Eng*, vol. 1231, no. 1, p. 012012, Feb. 2022, doi: 10.1088/1757-899x/1231/1/012012.
- [15] V. A. Ganesh, A. S. Nair, H. K. Raut, T. M. Walsh, and S. Ramakrishna, “Photocatalytic superhydrophilic TiO₂ coating on glass by electrospinning,” *RSC Adv*, vol. 2, no. 5, pp. 2067–2072, Mar. 2012, doi: 10.1039/c2ra00921h.
- [16] M. Shahhosseinia, S. Bazgir, and M. D. Joupari, “Fabrication and investigation of silica nanofibers via electrospinning,” *Materials Science and Engineering C*, vol. 91, pp. 502–511, Oct. 2018, doi: 10.1016/j.msec.2018.05.068.
- [17] K. Sun, L. Lu, Y. Jiang, Y. Wang, K. Zhou, and Z. He, “Integrated effects of PM_{2.5} deposition, module surface conditions and nanocoatings on solar PV surface glass transmittance,” *Renewable and Sustainable Energy Reviews*, vol. 82. Elsevier Ltd, pp. 4107–4120, Feb. 01, 2018. doi: 10.1016/j.rser.2017.10.062.
- [18] G. G. Jang, D. B. Smith, G. Polizos, L. Collins, J. K. Keum, and D. F. Lee, “Transparent superhydrophilic and superhydrophobic nanoparticle textured coatings: Comparative study of anti-soiling performance,” *Nanoscale Adv*, vol. 1, no. 3, pp. 1249–1260, 2019, doi: 10.1039/c8na00349a.

- [19] W. Zhao and H. Lu, "Self-cleaning performance of super-hydrophilic coatings for dust deposition reduction on solar photovoltaic cells," *Coatings*, vol. 11, no. 9, Sep. 2021, doi: 10.3390/coatings11091059.
- [20] D. Goossens, "Wind tunnel protocol to study the effects of anti-soiling and anti-reflective coatings on deposition, removal, and accumulation of dust on photovoltaic surfaces and consequences for optical transmittance," *Solar Energy*, vol. 163, pp. 131–139, Mar. 2018, doi: 10.1016/j.solener.2018.01.088.
- [21] A. Kumar, V. K. Saxena, R. Thangavel, and B. K. Nandi, "A dual effect of surface roughness and photocatalysis of crystalline TiO₂-thin film for self-cleaning application on a photovoltaic covering glass," *Mater Chem Phys*, vol. 289, Sep. 2022, doi: 10.1016/j.matchemphys.2022.126427.
- [22] V. T. Lukong, R. T. Mouchou, G. C. Enebe, K. Ukoba, and T. C. Jen, "Deposition and characterization of self-cleaning TiO₂ thin films for photovoltaic application," *Mater Today Proc*, vol. 62, pp. S63–S72, Jan. 2022, doi: 10.1016/j.matpr.2022.02.089.
- [23] M. A. M. L. de Jesus, G. Timò, C. Agustín-Sáenz, I. Braceras, M. Cornelli, and A. de M. Ferreira, "Anti-soiling coatings for solar cell cover glass: Climate and surface properties influence," *Solar Energy Materials and Solar Cells*, vol. 185, pp. 517–523, Oct. 2018, doi: 10.1016/j.solmat.2018.05.036.
- [24] N. Chundi, E. Ramasamy, S. Koppoju, S. Mallick, A. Kottantharayil, and S. Sakthivel, "Quantum-sized TiO₂ particles as highly stable super-hydrophilic and self-cleaning antisoiling coating for photovoltaic application," *Solar Energy*, vol. 258, pp. 194–202, Jul. 2023, doi: 10.1016/j.solener.2023.04.062.
- [25] R. J. Isaifan *et al.*, "Improved Self-cleaning Properties of an Efficient and Easy to Scale up TiO₂ Thin Films Prepared by Adsorptive Self-Assembly," *Sci Rep*, vol. 7, no. 1, pp. 1–9, 2017, doi: 10.1038/s41598-017-07826-0.

Chapter: 6 Conclusion and Recommendations

6.1. Conclusion

In this work, optically transparent, hydrophilic self-cleaning TiO₂-SiO₂ nanofibrous coatings were successfully developed via electrospinning on PV glass cover. Our results indicate that the optimal ratio for achieving self-cleaning effect is (1:1). Comprehensive analysis of structural and morphological properties confirmed the formation of desired anatase structure and nanofibrous morphology with fiber diameters ranging from 70-85nm. The coating maintained good optical transmittance of 86.9% in the visible region making it suitable for solar application. The developed coatings were soiled in an indoor soiling chamber to study the effect on soiling density, transparency, and photovoltaic properties under three different tilt angles 0°, 33.4°, and 60°. The study revealed that the randomly oriented networked structure of fibers combining with hydrophilic nature (WCA=11.3°) reduced the soiling density up to 38.9%, and 64.9% in comparison to uncoated substrate that showed 9.08%, and 22.2% for tilt 33.4° and 60° respectively. Furthermore, improvements of 16.1% and 16.5% in transmittance, and 0.8% and 2.6% in photovoltaic performance were observed for tilt angles of 33.4° and 60° respectively. These results show that electrospun TiO₂-SiO₂ nanofibrous coatings have a potential to increase solar efficiency by reducing soil accumulation even without water showering and enhancing self-cleaning capabilities.

6.2. Recommendations

The following future recommendations aim to address key areas of interest and explore new opportunities in the development and application of TiO₂-SiO₂ nanofibrous thin films for self-cleaning application in photovoltaics.

1. The effectiveness of the coatings can be further studied under different temperature, humidity, wind speed and water showering conditions.
2. To evaluate the stability and efficiency of anti-soiling coatings under diverse environmental circumstances, long-term durability tests must be conducted. It will be helpful to assess their performance over lengthy periods of time,

- including exposure to various weather conditions, dust kinds, and cleaning cycles, in order to determine their long-term viability and maintenance needs.
3. In order to improve the composite materials' anti-soiling capabilities, future research might concentrate on improving the composition and ratio of the components. Finding new ways to combine TiO_2 and SiO_2 , as well as additional chemicals or nanostructures, might provide coatings that function even better.
 4. The effect of electrospinning parameters such as flow rate, voltage, needle to collector distance can be studied to analyze the change in optical properties and wettability of the nanofibrous films.
 5. For scalability, the coatings can be developed on large area substrates which will enable commercialization and widespread adoption of the technology.
 6. For practical application, the coating materials' and production processes' cost-effectiveness must be considered. For their broad implementation in the solar energy sector, investigating cost-effective production processes and employing affordable and abundant materials would be essential.

Summary

The conclusion and suggestions for the creation and use of hydrophilic, self-cleaning, optically transparent TiO_2 - SiO_2 nanofibrous coatings on PV glass covers are given in this chapter. The study produced coatings with an anatase structure and a nanofibrous shape that had a (1:1) TiO_2 - SiO_2 ratio. The coatings showed reduced soiling density, enhanced photovoltaic performance, and high optical transmittance. The analysis's conclusion emphasizes how these coatings might boost solar efficiency by lowering dirt buildup and improving self-cleaning properties. Future research should investigate the efficacy of coatings in various environmental settings, carry out tests on long-term durability, enhance component composition and ratio, examine the impact of electrospinning parameters, develop coatings on large-area substrates for scalability, and take cost-effectiveness in manufacturing processes and materials into account for practical application in the solar energy sector.

Appendix-A: Journal Article

Self-Cleaning study of SiO₂ modified TiO₂ nanofibrous thin films prepared via Electrospinning for application in Solar cells

Izzah Batool^a, *Nadia Shahzad^a, Roha Shahzad^a, Aamir Naseem Satti^a, Rabia Liaquat^a, Adeel Waqas^a, Muhammad Imran Shahzad^b

^a*U.S.-Pakistan Center for Advanced Studies in Energy (USPCAS-E), National University of Sciences and Technology (NUST), H-12 Sector (44000) Islamabad, Pakistan*

^b*Nanosciences and Technology Department (NS&TD), National Centre for Physics (NCP), (44000) Islamabad, Pakistan*

*Corresponding Author's Email: nadia@uspcase.nust.edu.pk

*Corresponding Author's Postal Address: USPCAS-E Building, Ground Floor, Sector H-12, Islamabad 44000, Pakistan

Abstract

Optically transparent, hydrophilic Silica (SiO₂) modified Titania (TiO₂) nanofibrous thin films have been synthesized on glass substrates via using electrospinning technique for self-cleaning application in a solar cell. The coatings were prepared by varying the TiO₂-SiO₂ ratio as (3:1, 1:1, 1:3). TiO₂-SiO₂ formulated ratio (1:1) outperformed in comparison to other formulations and was found to have a crystalline nature with randomly orientated network of fibers having diameter in the range 88-95nm. FTIR spectroscopy confirms complete evaporation of polyvinylpyrrolidone (PVP) from temperature annealed sample. The electrospun TiO₂-SiO₂ (1:1) nanofibers showed hydrophilic nature with water contact angle (WCA) of 11.3°. The Soiling study was performed under different tilt angles of 0°, 33.4° and 60°. Upon soiling the coating showed >16% enhancement in optical transmittance than the glass substrate. Soiling density decreased up to 38.9%, and to 64.9% in comparison to uncoated substrate that showed 9.08%, and 22.2% and the photovoltaic (PV) efficiency was improved by 0.8% and 1% for tilt angles of 33.4° and 60° respectively.

Keywords: Self-cleaning, TiO₂-SiO₂, Hydrophilic, Electrospinning, Solar cells